1969-5

A Study of Turbulent Heat Transfer from a Flat Plate with Transverse Temperature Variations

John C. W. Kwan
Brigham Young University - Provo

A STUDY OF TURBULENT HEAT TRANSFER FROM A FLAT PLATE WITH TRANSVERSE TEMPERATURE VARIATIONS

A Thesis

Presented to the

Department of Mechanical Engineering Science

Brigham Young University

In Partial Fulfillment

of the Requirements for the Degree

Master of Science

by

John C. W. Kwan

May 1969

This thesis by John C. W. Kwan, is accepted in its present form by the Department of Mechanical Engineering Science of Brigham Young University as satisfying the thesis requirement for the degree of Master of Science.

May 14, 1969
(Date)

DEDICATION

To:

My parents

My beloved Shang

My brother Peter

ACKNOWLEDGEMENTS

The author wishes to express his appreciation to Dr. Howard S. Heaton for his many hours of counsel and advice, to Dr. Richard D. Ulrich and Dr. John N. Cannon for their helpful suggestions, to Bill Hays for his technical assistance. Gratitude is also expressed for the apparatus help of Mr. Marlo Anderson.

At last but not the least, the author would like to take this opportunity to thank Philip Lin for his cooperation in working through the experiment.

TABLE OF CONTENTS

LIST OF ILLUSTRATIONS

NOMENCLATURE

A = Area, surface area

h = Convective heat transfer coefficience, in BTU/hr. ft.^{2} $^\circ$F

i = Electrical current in amperes

k = Thermal conductivity in BTU/hr. ft. $^\circ$F

"l" = Mixing length

L = Length

n = Slopes of Nusselt - Reynolds Number plots

Nu = Nusselt Number for temperature-dependent-property solution

Nu_{cp} = Nusselt Number for constant-property solution

p = power in watts

p = pressure difference measured for velocity computations

p = Ambient pressure

Pr = Prandtl Number, defined as $Pr = uC_p/k$

q = heat rate in BTU/hr.

q_{net} = Heat rate from model surface, BTU/hr.

$= q_{in} - q_{total\ loss}$

Re = Reynolds Number based on the characteristic length of the model

T = Temperature in $^\circ$F or $^\circ$R

T_∞ = Ambient Temperature in ^oF or ^oR

T_p = Plate or strip temperature in ^oF or ^oR

U = Free stream air velocity in feet per sec.

β = Angular segment

ξ = Unheated starting length

ρ_{air} = Density of air

μ = Dynamic viscosity coefficient

CHAPTER I

INTRODUCTION

Heat transfer in turbulent flow from external surfaces has been investigated extensively in the past. Most of the theoretical and experimental work deals with a two dimensional boundary layer on isothermal or uniform heat flux surfaces with longitudinal temperature variation. However, little attention has ever been paid to the case in which the temperature of the plate varies transversely. This is a three dimensional problem due to the spanwise variation of the thermal boundary layer. The most elementary example of this is the boundary formed by the sudden temperature impulse that acts transversely across a flat plate as shown in Fig. 1. Theoretically, this spanwise boundary increases the heat transfer coefficient. A knowledge of this is important in the field of heating and cooling system design. It is also important for the investigation of spot-heat flux measurement.

The purpose of this thesis is to study this spanwise boundary effect on heat transfer in turbulent flow from uniformly heated strips on a large plate. This spanwise boundary effect will be designated

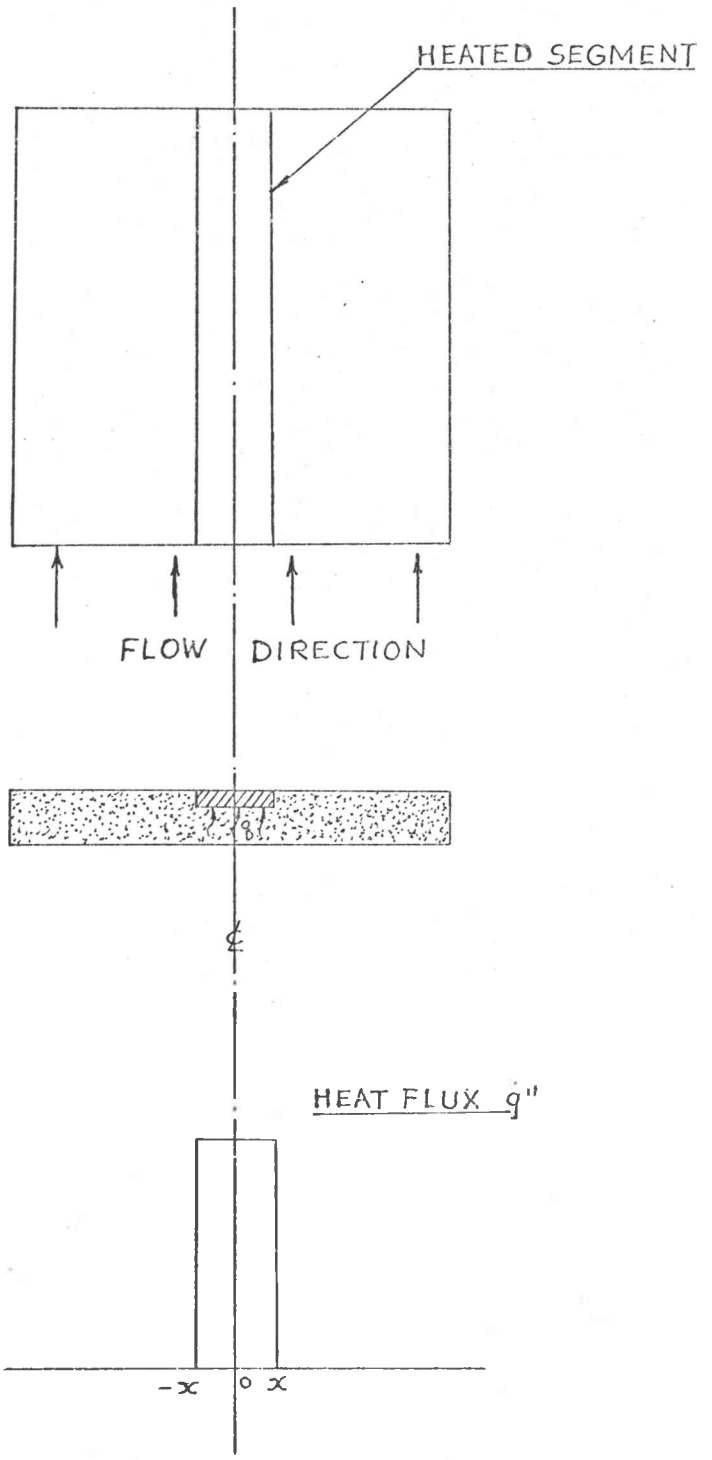

Fig. 1.--Plate with heated segment centered at X = 0

as the "edge effect."

In order to accomplish this research, one uniformly resistance-heated plate and five uniformly resistance-heated strips of different aspect ration (width to length ratio), each flush imbedded into an insulated foam plate, were used to simulate a plae with a transverse step temperature variation. The investigation was performed in a wind tunnel at a variety of speeds.

The experimental results were compared with a theoretical prediction for a flat plate having an unheated starting length.

CHAPTER II

SURVEY OF PREVIOUS WORK

In the past various experimental investigation and theoretical analyses have been undertaken to evaluate the heat transfer from plates and tubes under different heating conditions. Most of the work was done in solving problems in which the heat flux or temperature varied in the flow direction but was constant in the transverse direction. As an example, Sogin and Goldstein (7) (8) published a study of laminar and turbulent heat transfer from isothermal spanwise strips on a flat plate. In this study, naphthalen cast-in-trays was used to simulate the isothermal strips while the inert material between them simulated adiabatic strips.

There has been some work done showing the effect of transverse temperature variation in tube flow such as the theoretical study of heat transfer to fully developed laminar flow in a circular tube with arbitrary circumferential heat flux by Reynolds (11). In this study, Reynolds had taken the case of a tube with constant heat flux over a small portion of its circumference and insulated over the remainder as shown in Fig. 2. Reduction of this solution to the limiting case of

β = half angle of healed segment, radians

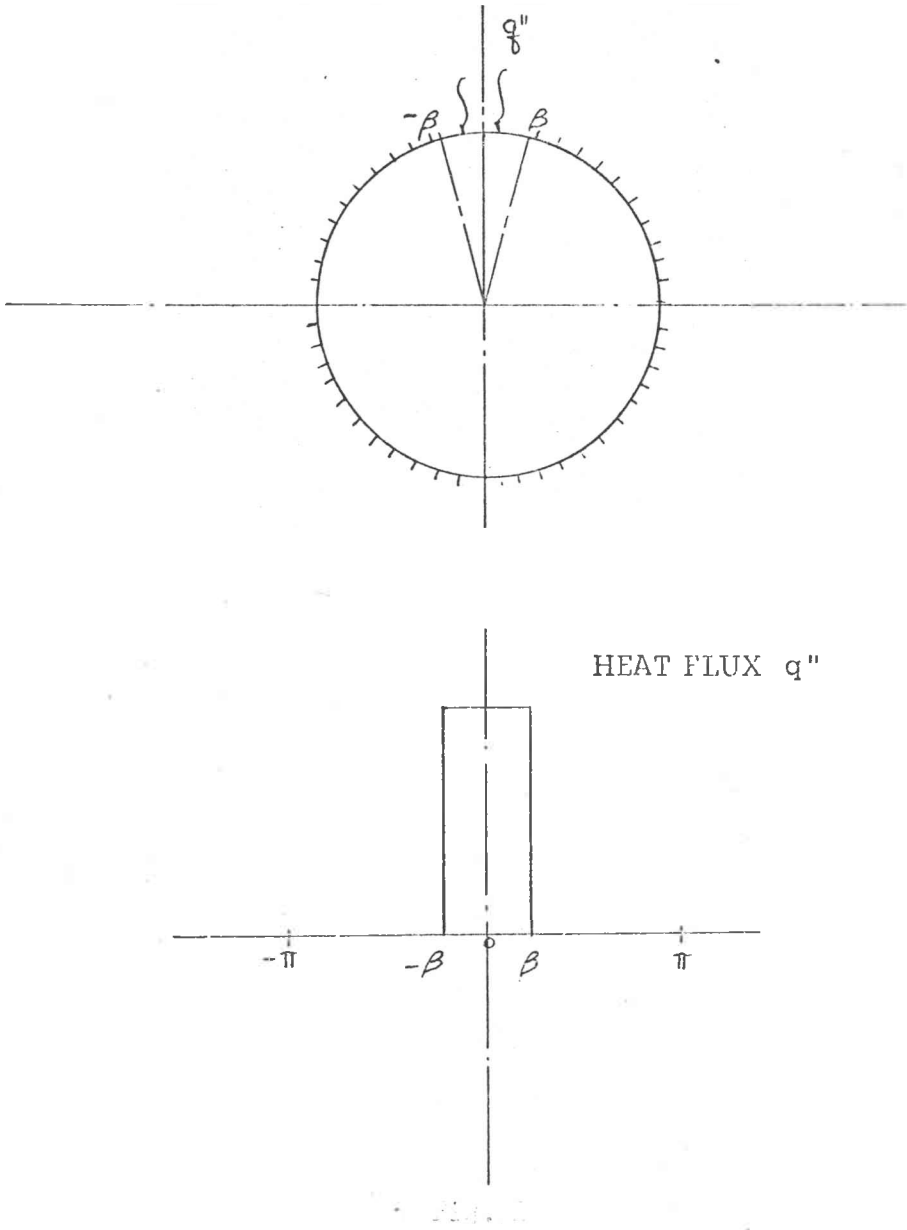

Fig. 2. -- Tube with heated segment centered at $\Theta = 0$

heating over a differential segment of circumference leads to a superposition kernel which in turn allows the arbitrary circumferential heat flux problem to be handled under the restriction of constant axial heat input. The results of this study are calculated and plotted with Nusselt number versus the width of the uniformly heated angular segment as shown in Fig. 3. From these results we see that the influence of circumferential heat flux on wall temperature is significant. Of particular interest in this study is that the narrower the heated region the higher the Nusselt number. This shows the nature of the edge effect.

Later, Reynolds (7) extended the above mentioned analysis to turbulent flow, in which he stressed that the effects of circumferential heat flux variation in turbulent flow were sometimes more pronounced than in laminar flow. His analysis was based on the idealization that the eddy diffusivity for heat in radial and circumferential direction are identical. In this analysis the wall heat flux variation was expressed as a mean value, q''_o, plus a heat flux variation $F(\theta)$ about the mean:

$$q''_w(\theta) = q''_o + F(\theta)$$

The function $F(\theta)$ satisfied the relation

$$\int_0^{2\pi} F(\theta)\, d\theta = 0$$

Then $F(\theta)$ could be represented as a Fourier series to obtain an arbitrary variation in heat flux.

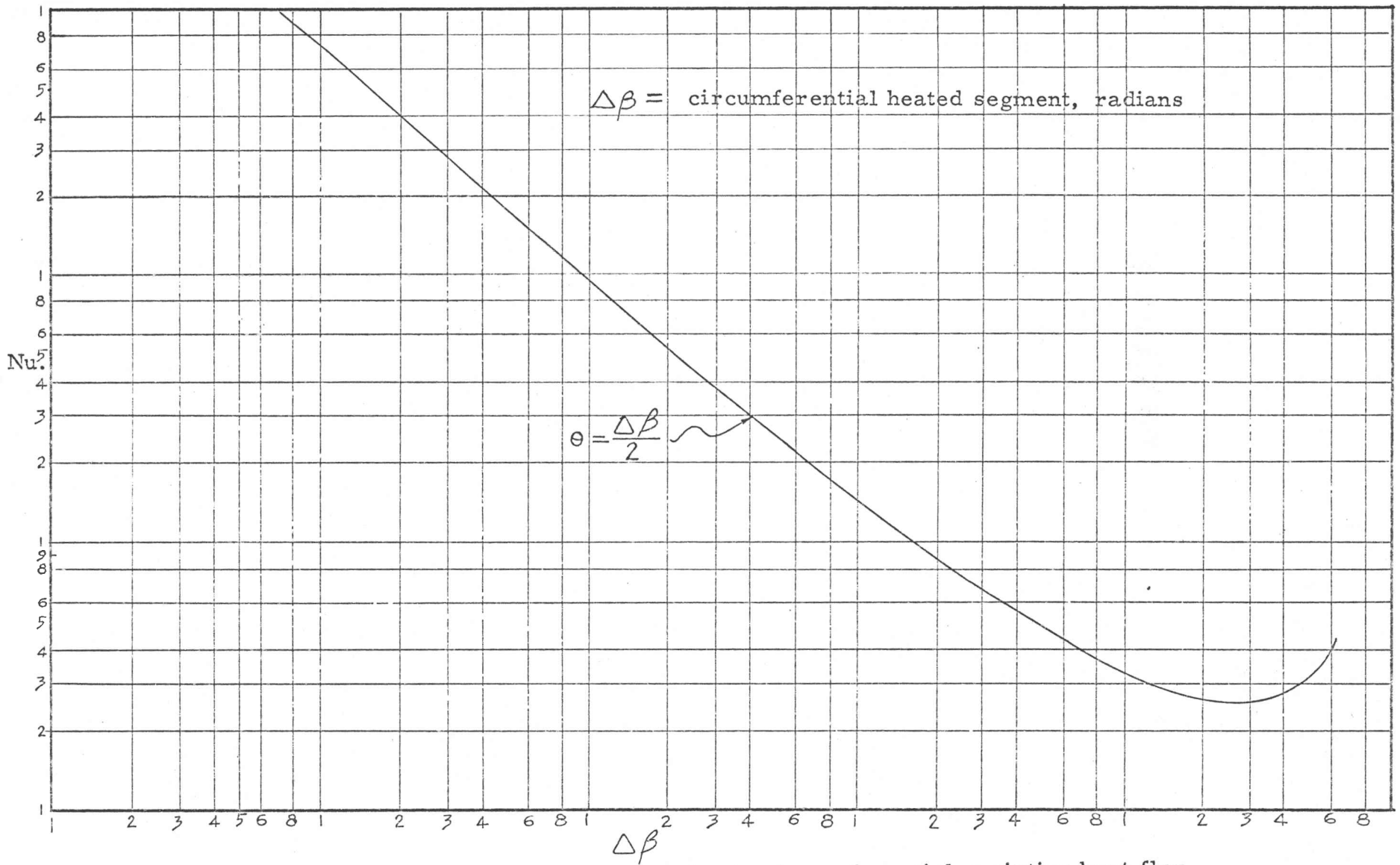

Fig. 3.--Nusselt number variation due to circumferential variation heat flux

At the same time, the problem of turbulent heat transfer in a tube with circumferential varying temperature or heat flux was studied by Sparrow and Lin (13).

Black and Sparrow (14) performed an experiment to determine the heat transfer characteristics for turbulent flow in a circular tube with circumferentially varying wall heat flux. The results indicated that the prediction of the prior analyses of Reynolds (12) and Sparrow and Lin (13) appear to overestimate the circumferential variation of the heat transfer coefficients, especially at high Reynolds numbers. Black and Sparrow (14) suspected that the discrepancy arose because of the assumption of equal turbulent diffusivities in the radial and tangetial directions. Through the study of this experiment, Sparrow and Black (14) found that in the neighborhood of the wall, the tangential turbulent diffusivity is greater than the radical turbulent diffusivity.

Although some information is available regarding the influence of circumferential heat flux variation on heat transfer to fully developed laminar and turbulent flow in a circular tube, there is still none regarding the edge effect of a longitudinal strip on a flat plate. The present work constitutes a study in this direction.

CHAPTER III

DESIGN AND CONSTRUCTION OF TEST SYSTEM

In the developing the heat transfer system to determine the edge effect experimentally, the following apparatus and equipment were utilized.

I. Subsonic wind tunnel and calming chamber

II. Insulation foam plates and mounting frame

III. Five, 6 inch long strips of different widths and a 6 inch square plate.

IV. Plate heaters

V. Inclined manometer

VI. Pitot tubes and thermocouples

VII. Auxiliary equipment

- A. D. C. power supply
- B. potentiometer
- C. voltmeter, ammeter, wattmeter and ohmmeter
- D. balance device

The arrangement of the above mentioned apparatus are shown in Fig. 4

and Fig. 5.

Wind tunnel

The wind tunnel used an open circuit with a D. C. fan at the outlet end. In order to prevent large scale turbulence from entering the tunnel nozzle a calming chamber (15) using cheese cloth, furnace filters and insect screen was attached to the inlet of the wind tunnel. The contraction ratio of the nozzle was approximately 8:1.

The test section of the wind tunnel had a 12 inch square cross section and was 22 inches in length. Both the vertical sides of the test section were made of acrylic plastic so that a visual observation of the test model was possible. The air speed was regulated by adjusting a variable resistance bank. The air speed varied from 20 feet per second to 105 feet per second.

Insulation foam plates and mounting frame

The frame was machined from oak, The design is shown in Fig. 6. Along both sides there were holes drilled for mounting the frame in the wind tunnel test section with metal screw fasteners. The leading edge was circular in shape to provide smooth boundary layer development without separation. A 1/4 inch by 1/4 inch trough was machined on the inside of the two side components of the frame.

The insulatpn foam plate was 11 inches by 11 inches by 3/4 inch. The details are shown in Fig. 7. A recess 6 inches long,

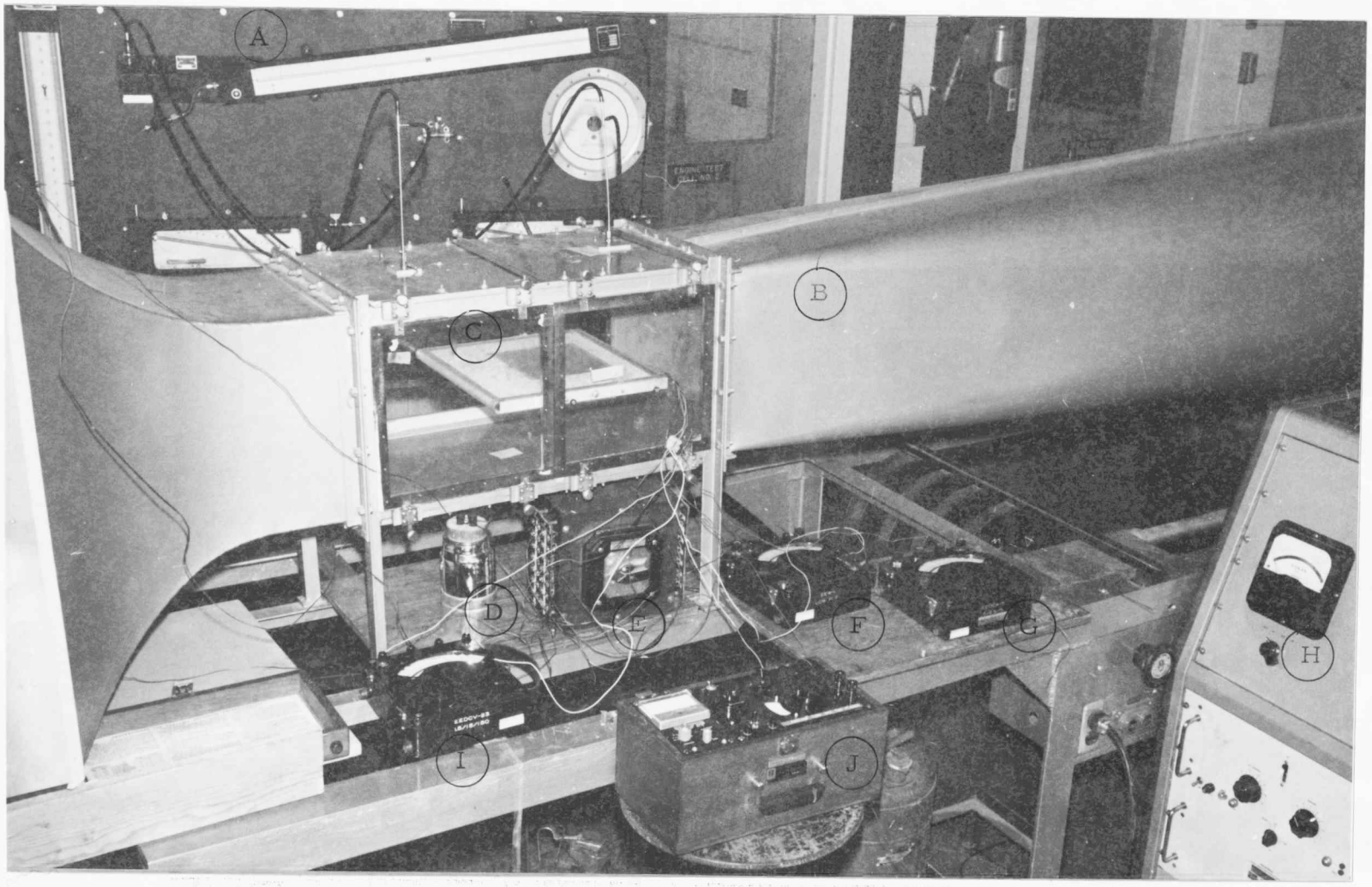

Fig. 4. --Test assembly I, showing (a) inclined manometer, (b) wind tunnel, (c) test model, (d) reference bath, (3) rotating tap switch, (f) wattmeter, (g) ammeter, (h) power supply, (i) voltmeter, (j) potentiometer

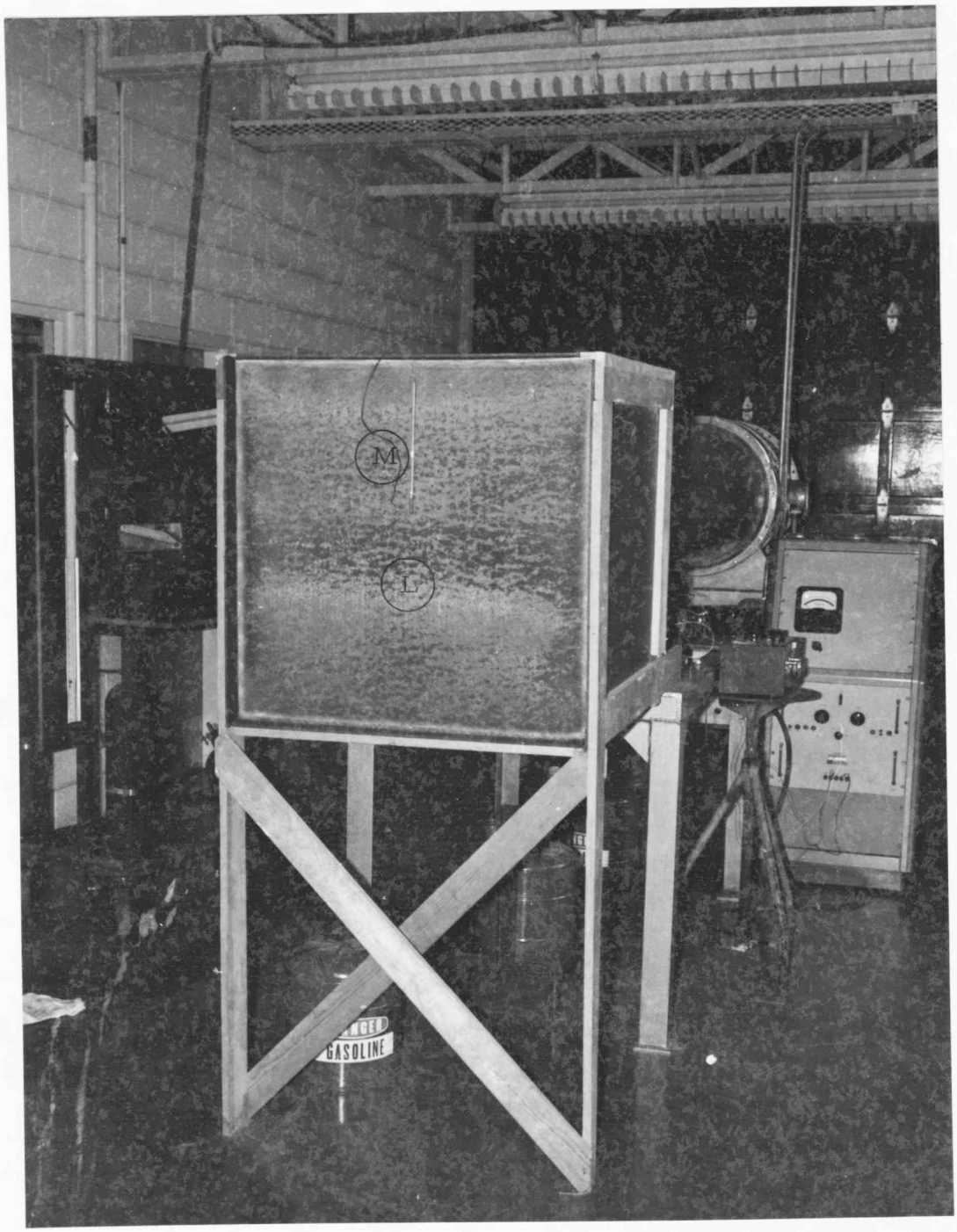

Fig. 5.--Test system II, (L) calming chamber, (M) thermocouple

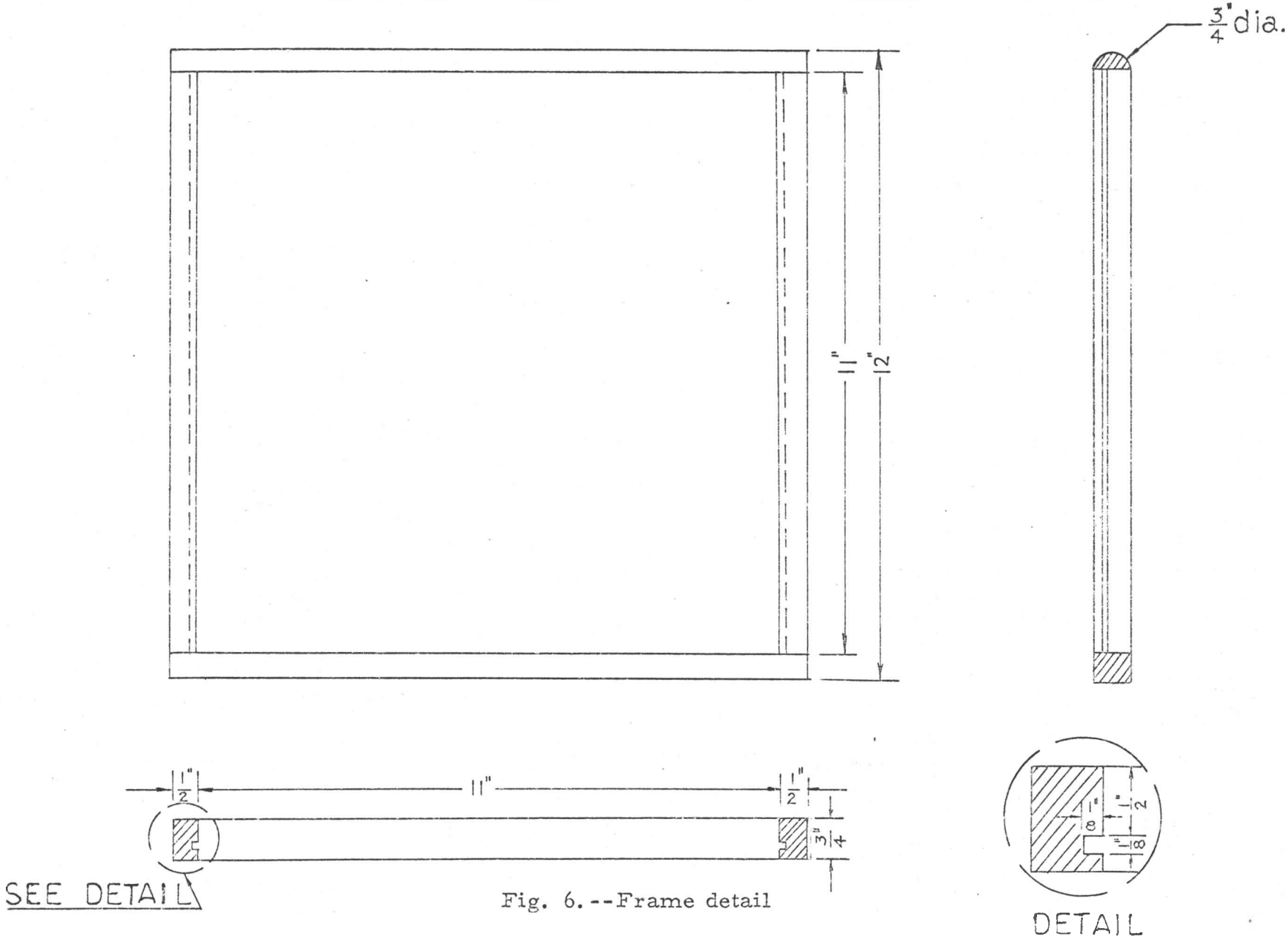

Fig. 6.--Frame detail

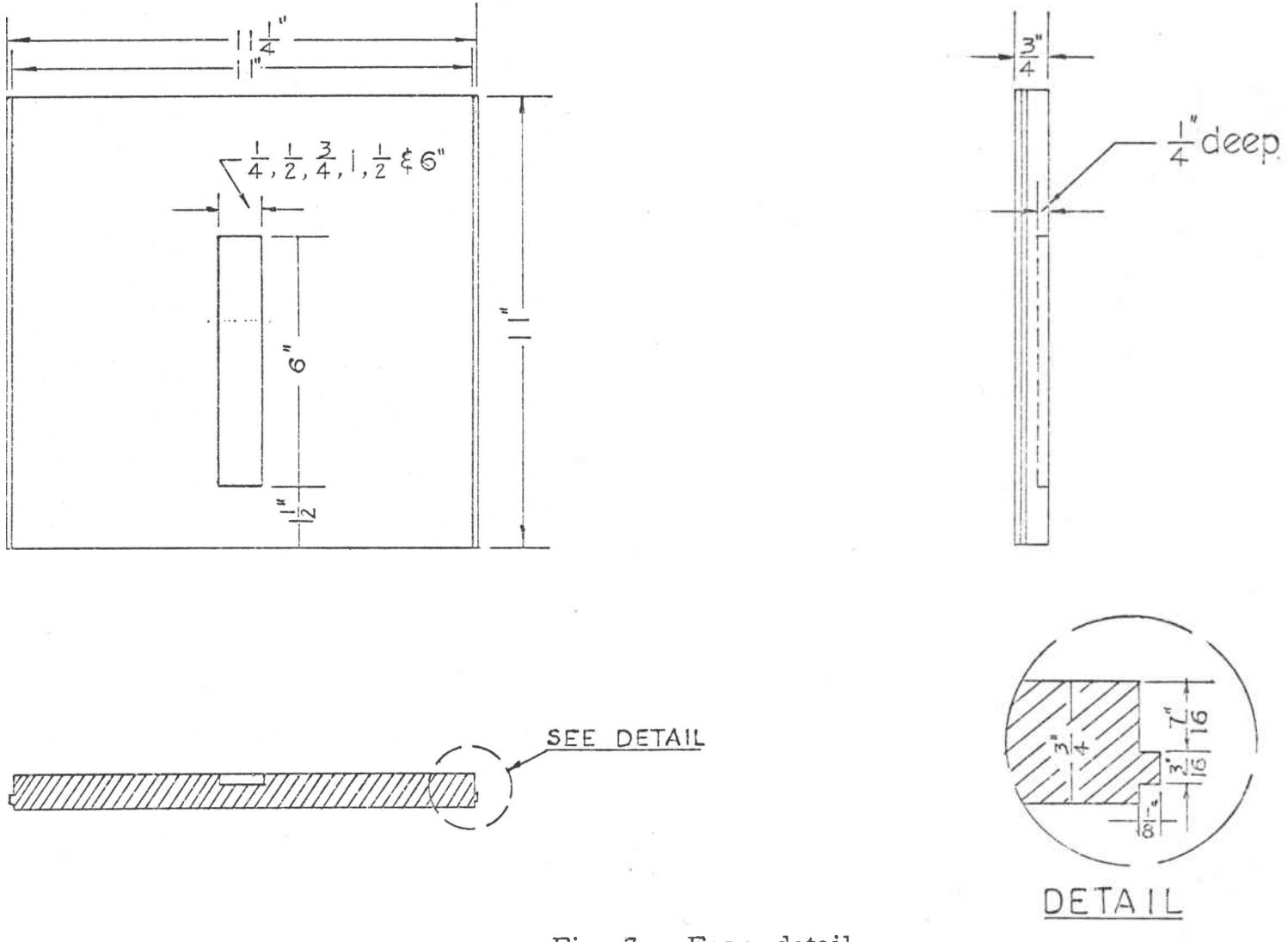

Fig. 7.--Foam detail

1/4 inch deep with a width corresponding to the widths of each of the aluminum strips was machined on each plate. A 1/8 inch by 1/4 inch eliptical hole was drilled through the center of the trailing edge for the power leads and thermocouples wires to come through from the test sample to the measuring devices and power source. The insulating foam plate was designed to allow at least one inch of insulating material surrounding and half inch of material underneath the test sample.

To insure that the top surfaces of the wooden frame and the insulating foam plate would be mounted flush, the side edge of the insulating foam plate was machined to slip fit into the wooden frame.

Test samples

The test samples included five 6 inch long strips with widths of 1/4 inch, 1/2 inch, 3/4 inch, 1 inch, and 1 1/2 inch and a 6 inch square plate. All of the test samples were 3/16 inch thick and were fabricated from commercial aluminum sheet. The aluminum was chosen to minimize the temperature gradient in all directions making it possible to attain a reasonably uniform surface temperature. A 1/16 inch hole was drilled into the side edge of the plate and strips for thermocouple installation. The surfaces of the plate and strips were sanded to a degree of smoothness that was felt to eliminate the roughness effect (16).

Plate heater

A heating element made from nichrome wire was located on the bottom of each strip and the square plate. To have reasonably uniform heat flux throughout the strips the heating wire was laid with equal spacing. A thin layer of electrical insulation cement was placed on the plate to prevent shorting of the nichrome wire.

The nichrome heating wire was attached to the plate by glass cloth electric tape (3-M product, No. 27). This tape was used because the bounding agent on the tape was a thermal setting material and the glass fabric backing had good high temperature properties. Each finished strip was tested before being installed in the foam plate for electrical short circuits. The details of the design are shown in Fig. 8.

A D. C. regulated power supply (Regatran Semiconductor power supply, Electronic Measurement Co.) with an output capacity of 0-50 volts at 0-15 amps. was used to supply power to the heater.

Instrumentation

Iron-Constantan thermocouples were used for all temperature measurements. The temperature distribution along the 6 inch by 6 inch plate was sensed by four thermocouples. The thermocouples were inserted about 1 3/4 inches into the four edges of the plate. Only one thermocouple was used to measure the strip temperature because of size limitation. Underneath the strips and the plate an additional

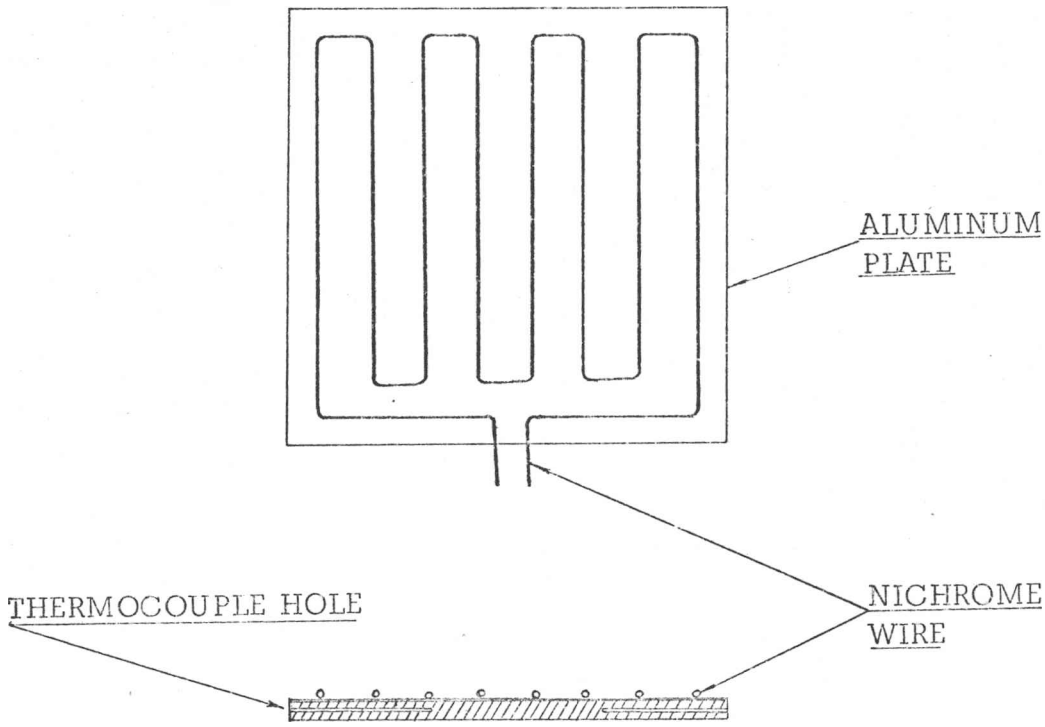

Figure 8.--Plate heater detail

thermocouple was affixed to sense the bottom temperature of the plate heater. The details are shown in Fig. 9. The temperature of air in the flow stream was sensed by two thermocouples. The electromotive force of the thermocouples was measured with a Honeywell potentiometer (model 2732). The thermocouple system was referenced to an ice-water bath. A rotating tap switch was used in the system not only to allow a single reference bath to be used but also to facillitate quick temperature measurement of all points in the system.

The air flow rate and pressure in the test section of the wind tunnel were metered by a pitot tube. The static pressure and kinetic pressure were read from a Merian inclined manometer. The atmospheric pressure was measured by a barometer.

The heater power was measured by a voltmeter and an ammeter. The reading was also checked by a wattmeter.

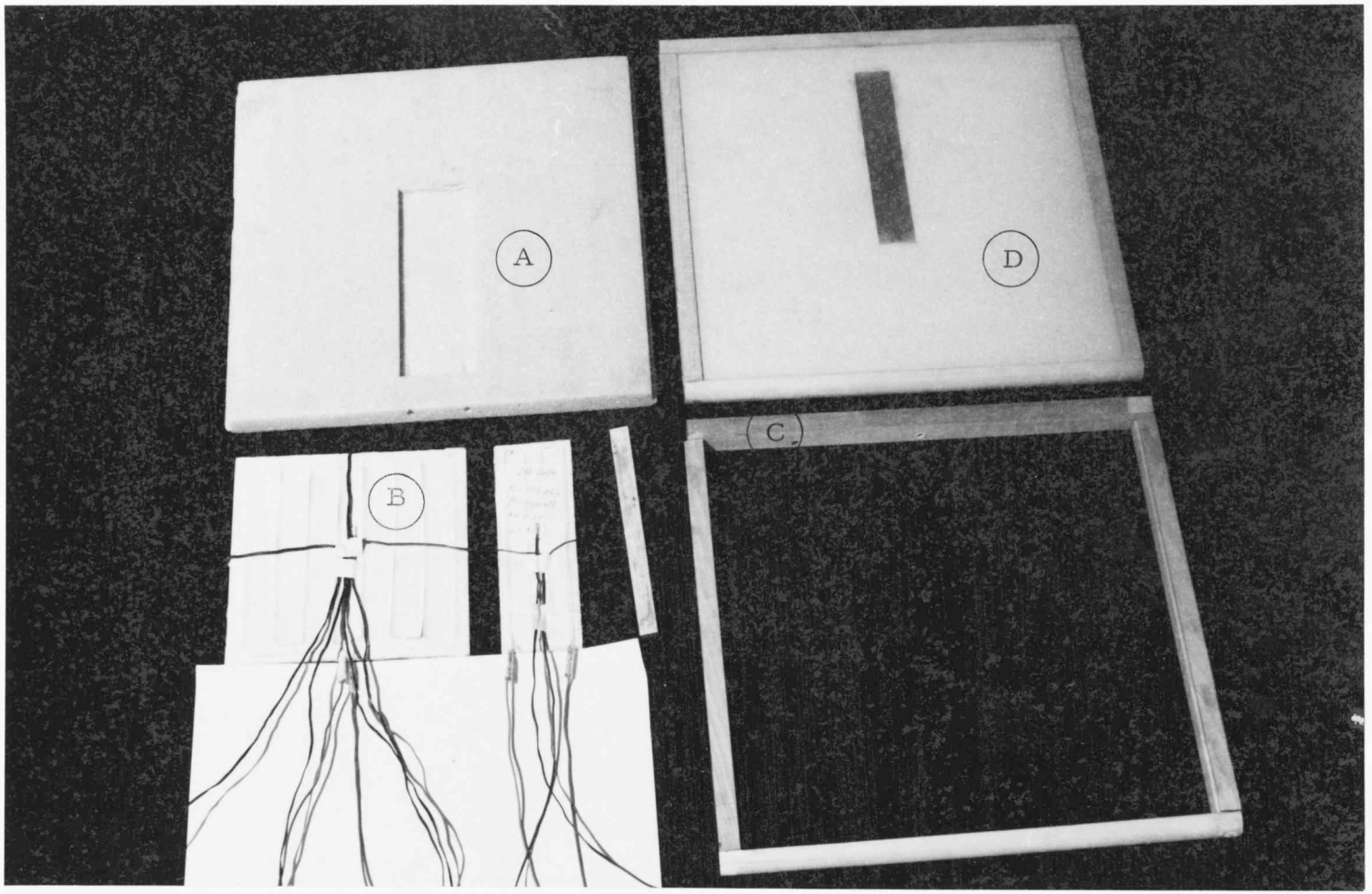

Fig. 9. -- Test sample, showing (a) insulating foam plate (b) plate and strips (c) wooden (oak) frame (d) assembled test model

CHAPTER IV

EXPERIMENTAL PROCEDURE

The following procedure was applied in the experiment to obtain the rate of heat transfer from the plate and strips.

After the plate and the strips were installed in the insulating foam plate as shown in Fig. 10 the whole test system was then mounted horizontally into the test section of the wind tunnel. A level was used to assure that the test system was being installed absolutely parallel to the flow as shown in Fig. 5. Having the wall panels secured properly in place and all the crevices firmly sealed with masking tape to eliminate the air leakage, the power supply for the electric heater and the wind tunnel motor were then turned on to establish the heat flux and flow stream, respectively.

The time required to reach the steady state was approximately two hours. Having the flow rate maintained at a constant speed and the power input to the heater regulated, the plate or the strip temperature was checked every ten or fifteen minutes until the temperature of the plate or the strip reached steady state. This steady state was assumed to have been reached at the time that the plate temperature remained

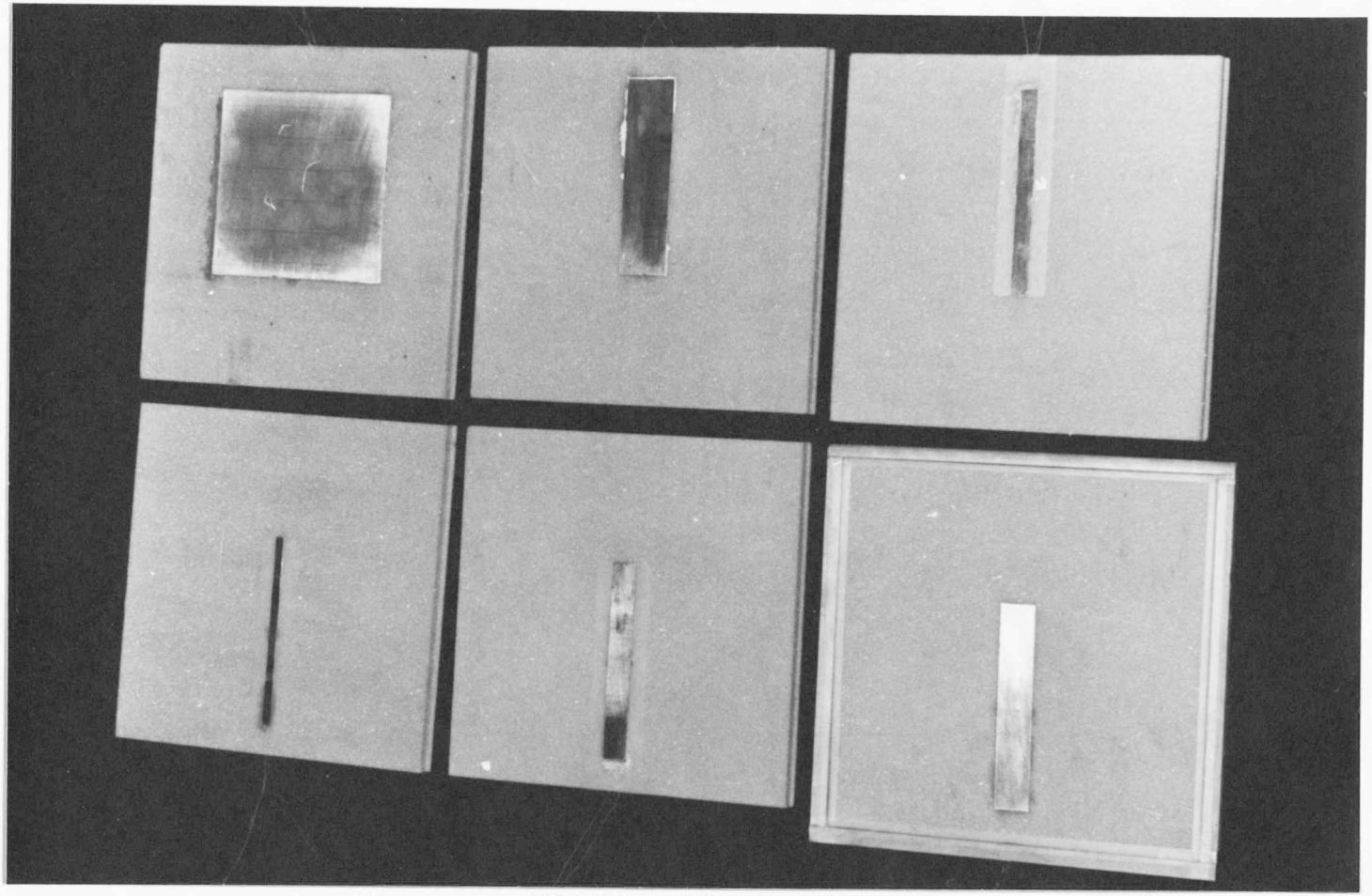

Fig. 10.--Test models

constant over a fifteen minute interval. The experimental variables, including thermocouple readings, manometer readings, power input reading and barometer pressure were then recorded each time after the plate or strip temperature achieved the steady state.

The power supplied to the strip heater was varied directly with the aspect ratio of the plate and the strips.

Because the environment for the test was relatively important, most of the experiments were run at night. This helped to eliminate some of the undesirable side effects of temperature fluctuations generally caused by machinery in operation. Before the experiment began, the environmental conditions were carefully adjusted where possible to reduce the variations in surrounding conditions such as the arrangement of the room heaters.

CHAPTER V

CALIBRATION OF INSTRUMENTS AND MEASUREMENT OF FOAM THERMAL CONDUCTIVITY

To minimize experimental error, both the thermocouples and the inclined manometer were calibrated before they were used. Also, the thermal conductivity of the insulating foam plate was measured.

The inclined manometer used in this experiment was calibrated with a Merian Model 34FB2TM micromanometer. The result of the calibration is shown in Fig. 11.

The thermocouple wire was calibrated with the ESI Model 1302 Thermometer Assembly. The assembly consisted of a platinum resistance thermometer, a ESI Model 300 PVB potentiometric voltmeter, a ESI Model 1303 thermometer adapter, a Rosemount Model 319A calibration bath, a Rosemount Model 911 constant temperature ice bath, and a Tronac Model PTC 100 temperature controller. The liquid used was Dow Corning 200 silicon liquid. The whole thermometer assembly provided an accuracy of $\pm$ 0.1^{o} C in the range of 20^{o} C-100^{o} C. The results of the thermocouple calibration is shown in Fig. 12.

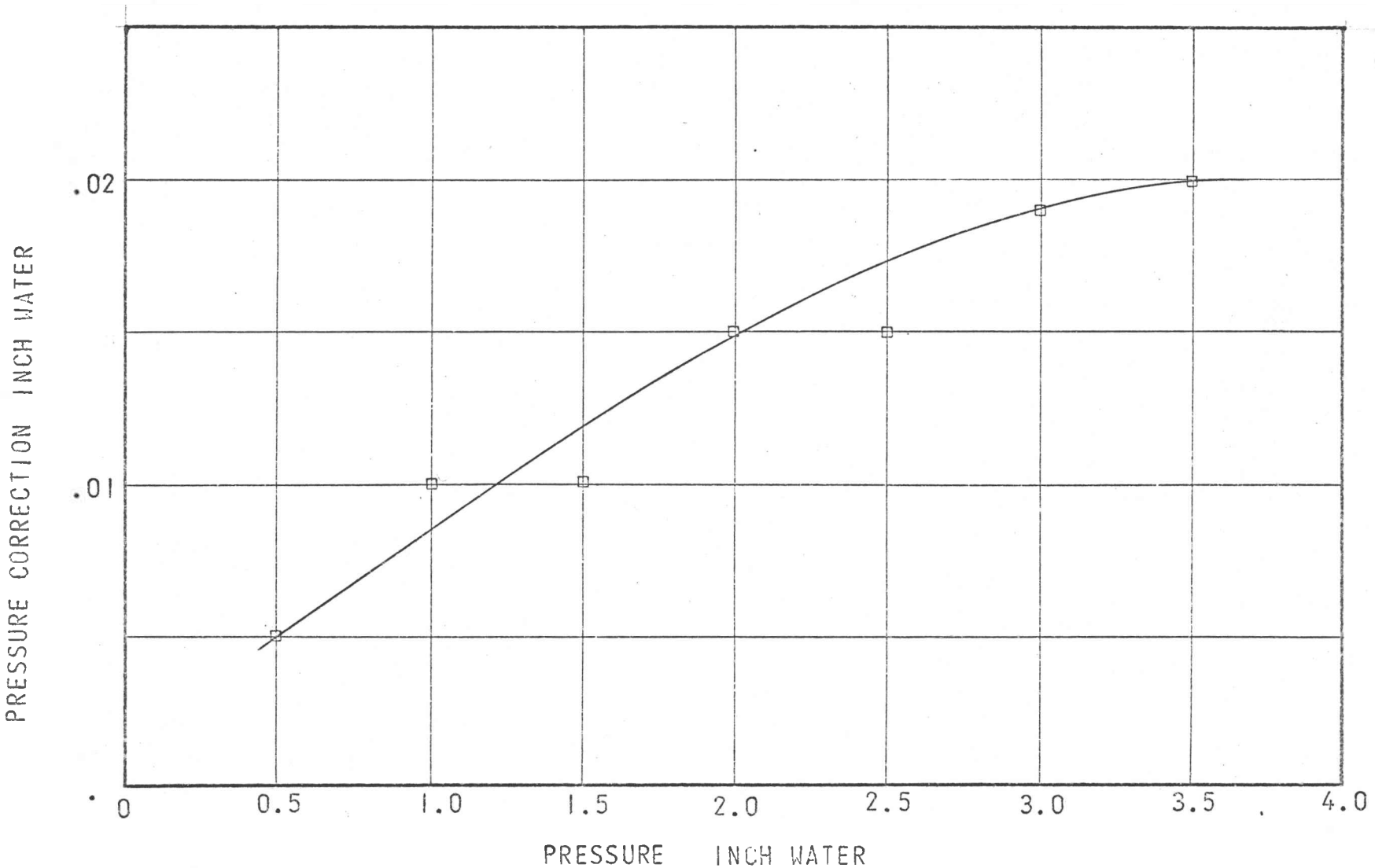

Fig. 11.--Manometer calibration curve

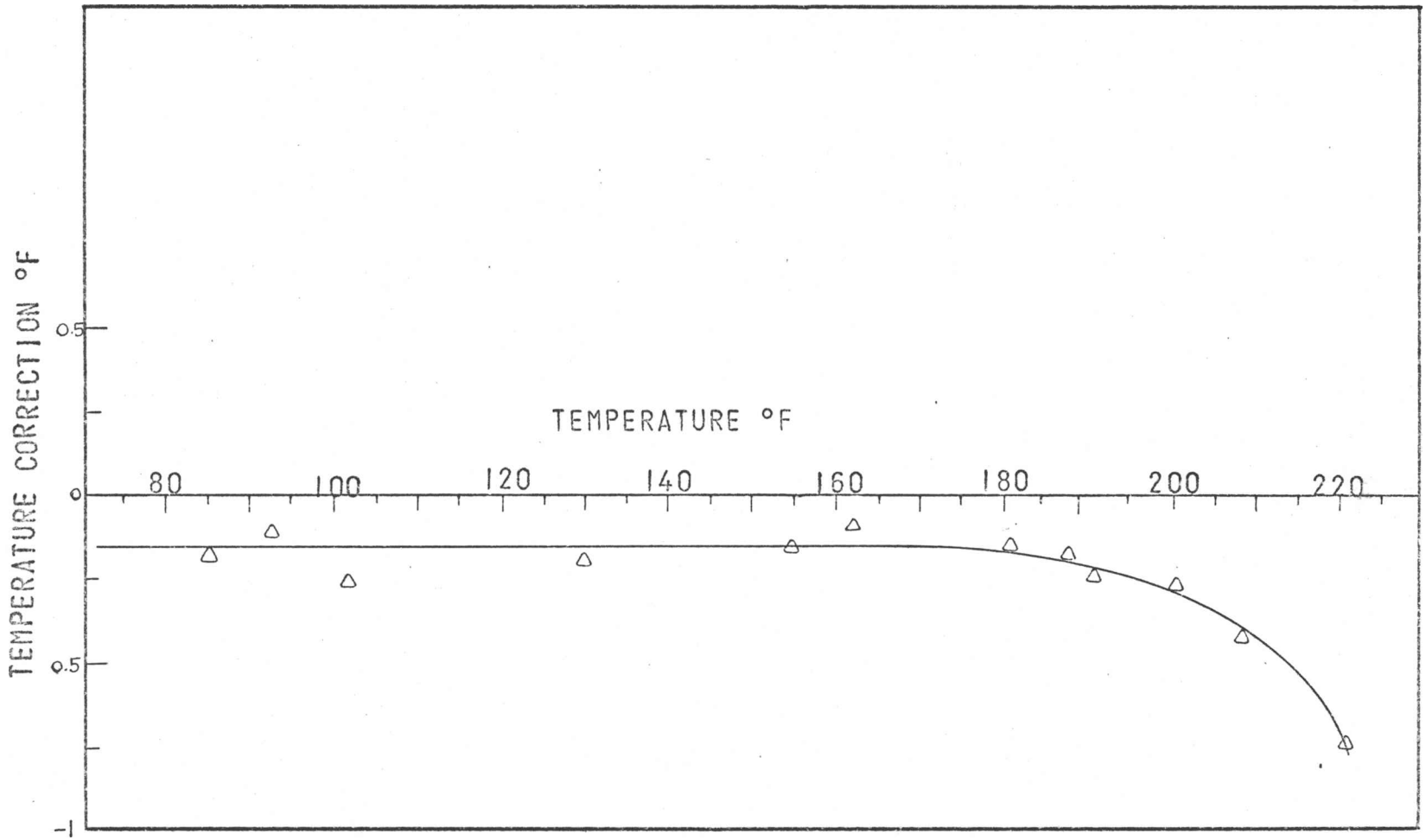

Fig. 12. --Thermocouple calibration curve

The apparatus used to determine the conductivity of the insulating foam plate is shown diagrammatically in Fig. 13. The test assembly consisted of sandwiching a flat electrically heated plate between two equally sized insulating foam plates. This sandwich like assembly was then clamped in between two 1/8 inch aluminum plates. Clamps were used to provide uniform pressure over the foam and maintain good surface contact. Thermocouples were used for temperature measurement. The detail of the test assembly is shown in Fig. 14.

Since the insulating foam plates were equal in thickness L, area A and thermal conductivity, and the rate of heat flow q from the heater was known by means of precise electrical measurement, the thermal conductivity was thus calculated according to the following equation

$$q/2 = KS\Delta T$$

where S is the geometric shape factor.

The shape factor of the foam plates used for the thermal conductivity measurement and the insulating foam plate in the major experiment were found by means of electrical analogy using a conductive paper model. In the experiment the boundary conditions corresponding to a constant temperature potential thermal model were obtained by applying copper wire and highly conductive silver paint to the surface of the paper and attaching them to direct-voltage source.

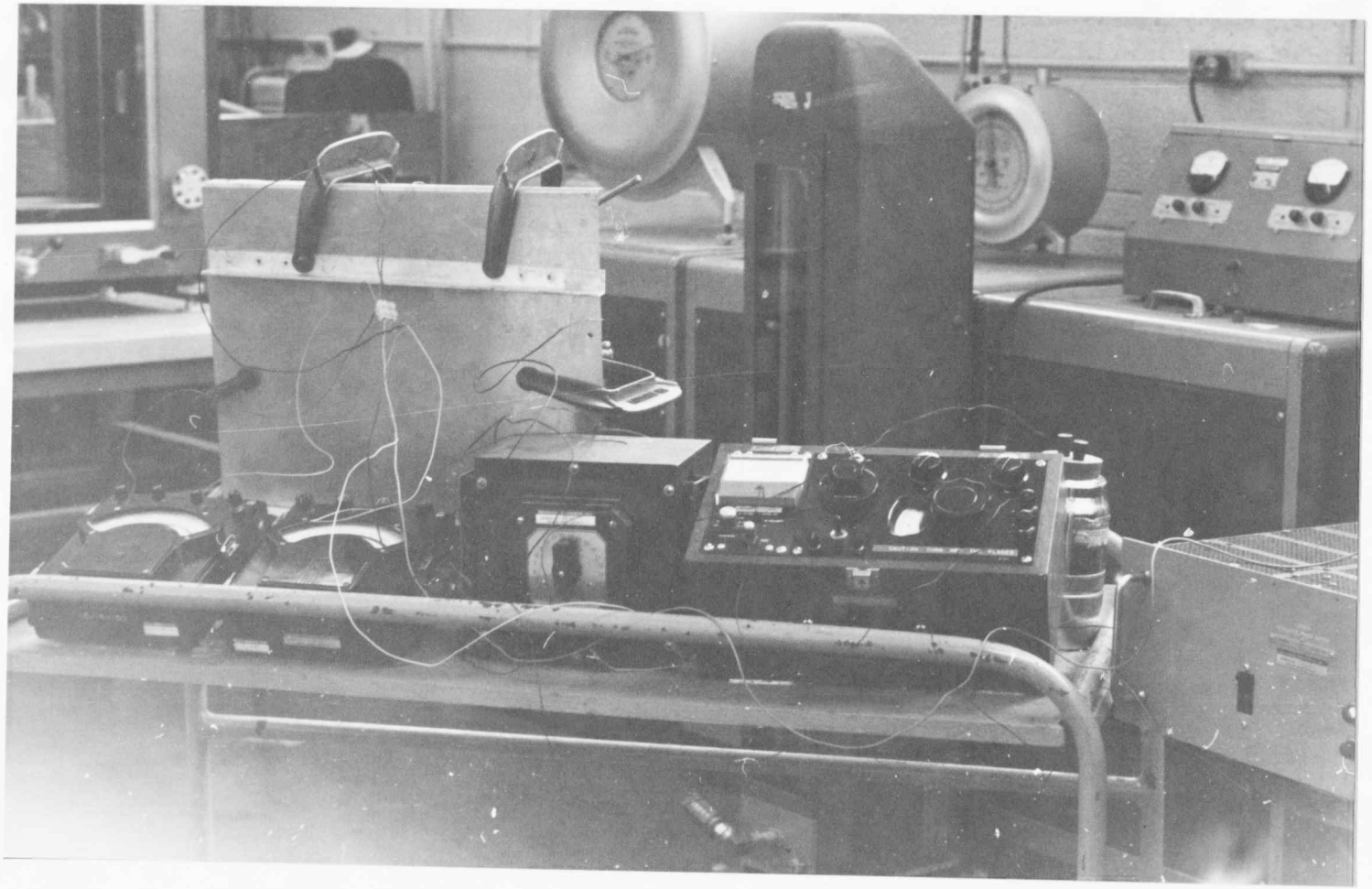

Fig. 13. -- Thermal conductivity measurement system

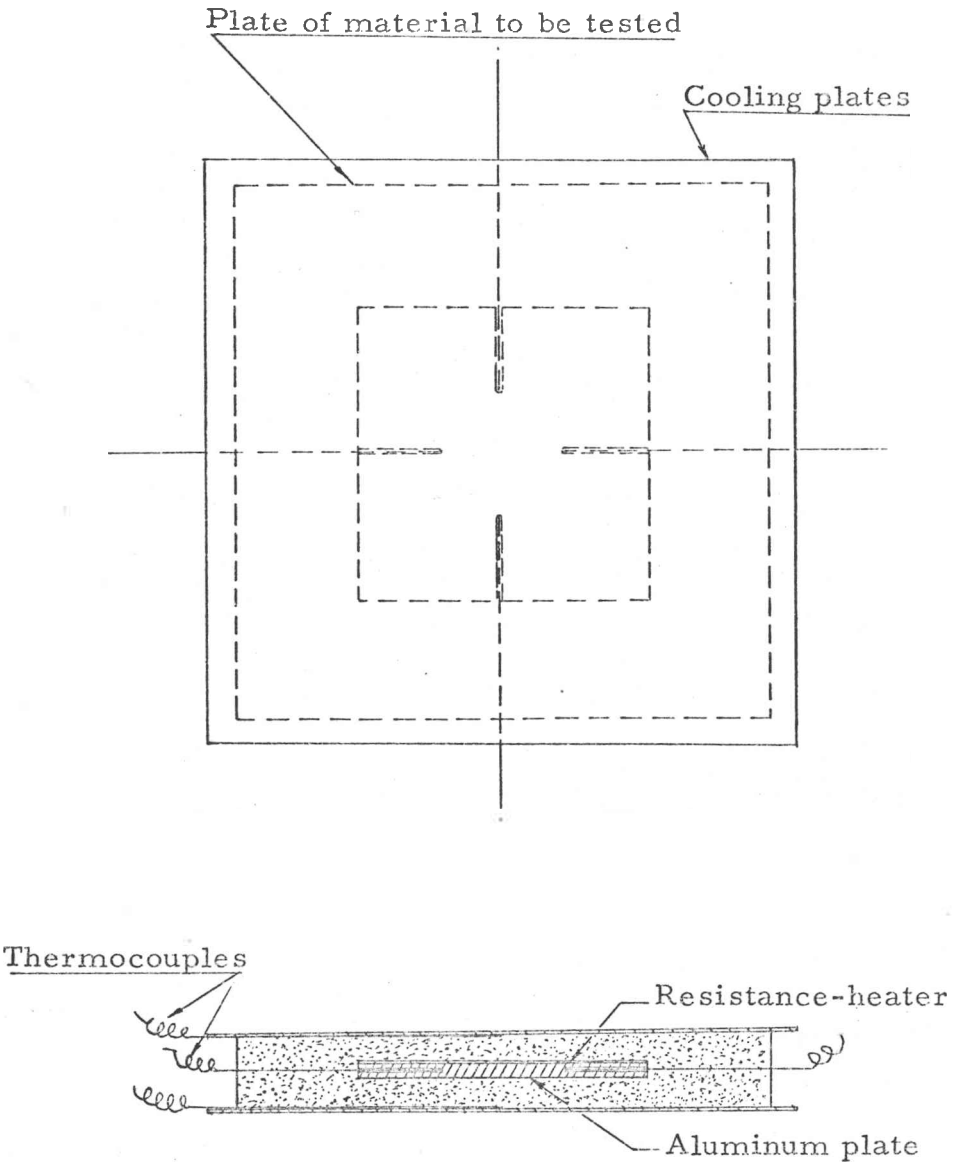

Fig. 14. --Thermal conductivity measurement assembly

The unpainted edges corresponded to the insulated surfaces in the thermal model. Recording the equipotential and flow lines was accomplished by means of a Simpson 311 Volt-Ohm-Ammeter as shown in Fig. 15. For the purpose of finding the significant heat conduction loss distance through the insulating foam plate an equal potential field was plotted as shown in Fig. 16. The result indicated that only the first half inch from the edge of the plate is significant. Hence the plate could be considered as end insulated. The method for calculating this is given in Appendix C. The calculated thermal conductivity was 0.0112 BTU/hr. ft. ^{o}F.

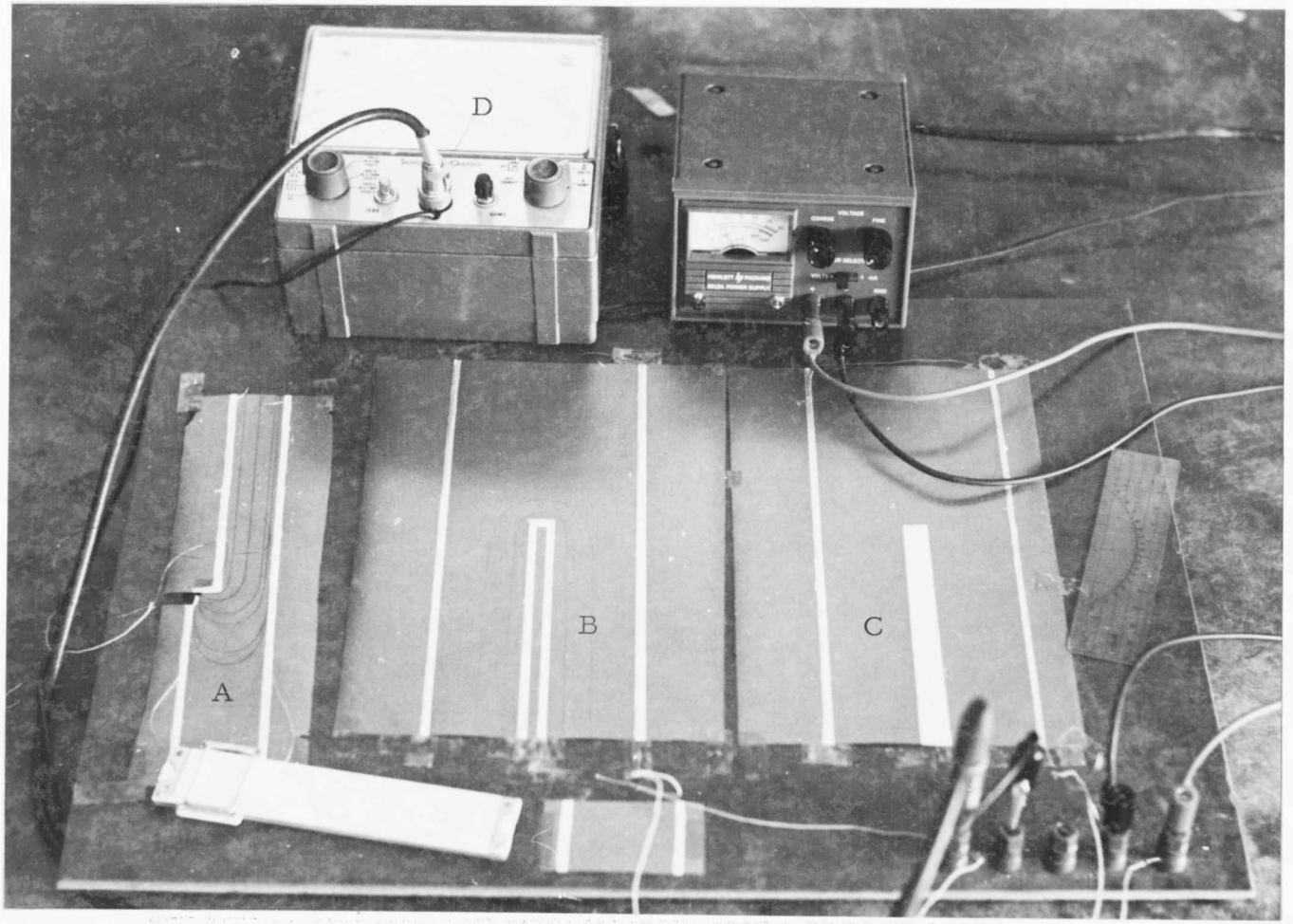

Fig. 15.--Electrical analogy by conductive sheet model showing (a) insulation plate model, (b) and (c) models used for thermal conductivity measurement, (d) ohmmeter, (e) rectangular model

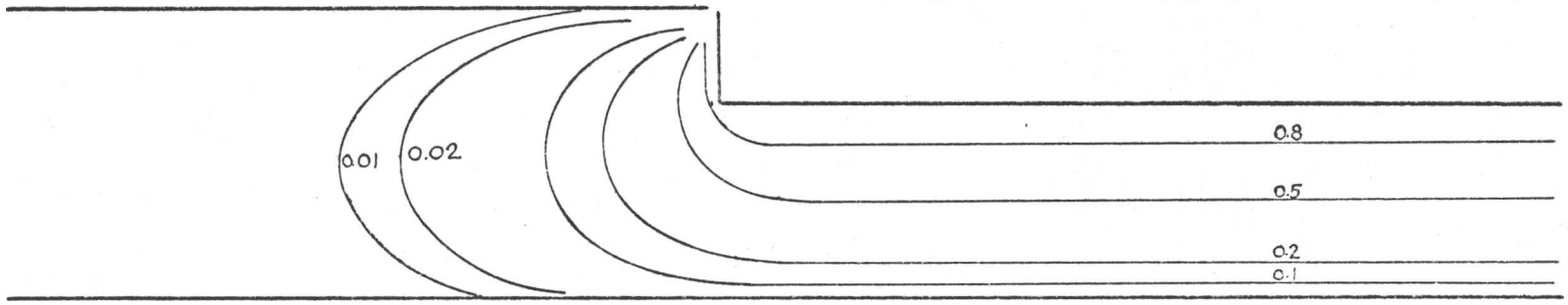

Fig. 16. Equal potential field of the insulating foam plate

CHAPTER VI

PRESENTATION AND DISCUSSION OF RESULTS

The effect of transverse temperature variation on heat transfer from a plate in turbulent flow was studied in this thesis. The study was accomplished with five uniformly heated strips of different aspect ratio and a 6 inch square plate each mounted in a 1 foot square insulating foam plate. The results are shown from Fig. 17-26 and Table 1-6.

The plots of Nusselt number as a function of Reynolds number for the individual strips are presented from Fig. 17 through Fig. 21. In the figures a comparison with the measured results of the 6 inch plate are also shown.

Shown in Fig. 22 is the Nusselt number versus Reynolds number plot of the 6 inch square plate, an analytical solution of turbulent heat transfer from a flat plate having an unheated starting length is also included. The analytical solution was worked out through equation

$$Nu = 0.0295\, Pr^{0.6} L^{-0.8} \left\{ \int_{\xi}^{L} \frac{1}{X^{0.2}} \left[1 - \left(\frac{\xi}{2\ell} \right)^{\frac{9}{10}} \right]^{-\frac{1}{9}} \right\} Re^{0.8}$$

The above equation was derived from (1).

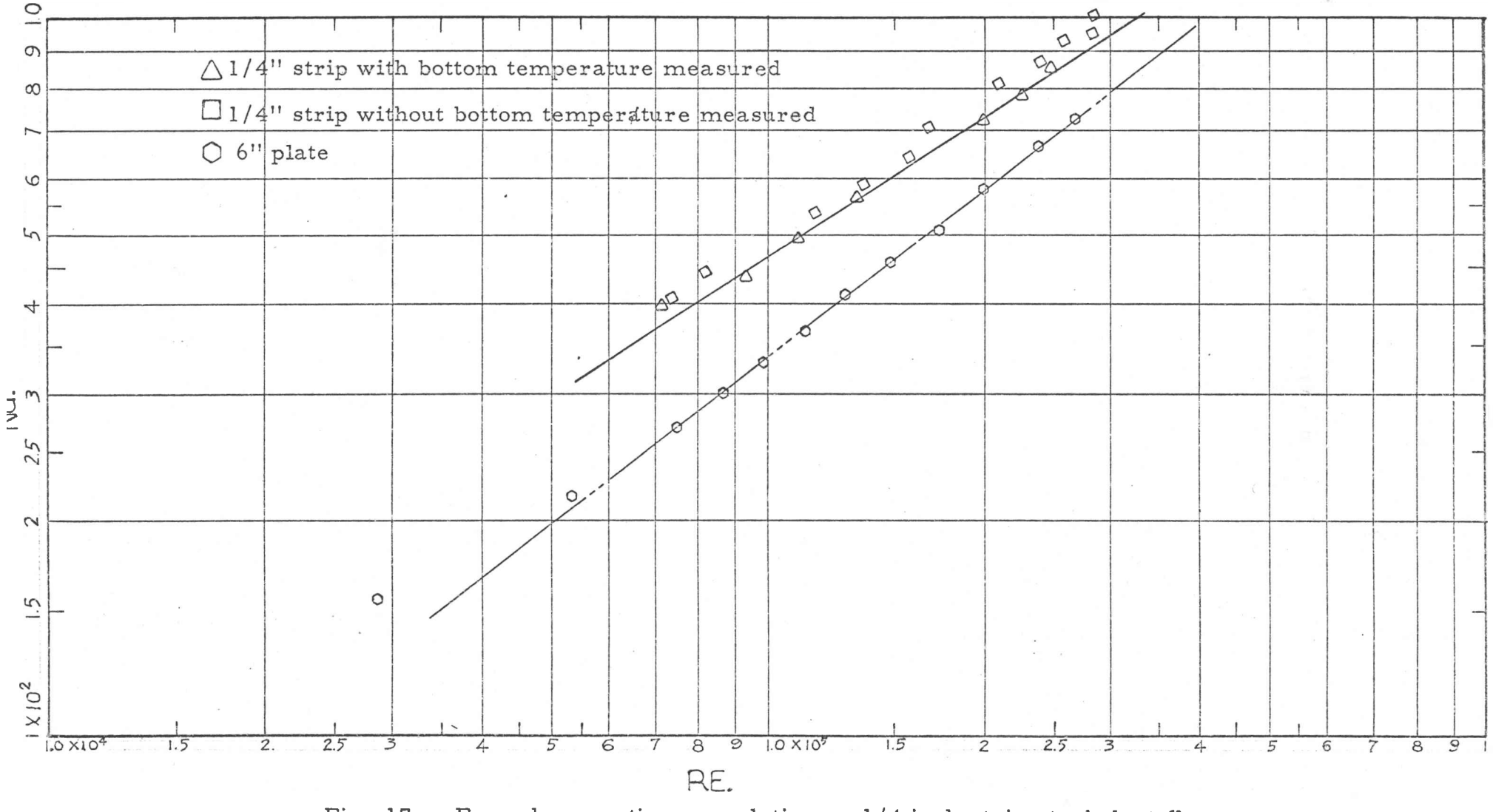

Fig. 17.--Forced convection correlation on 1/4 inch strip, turbulent flow

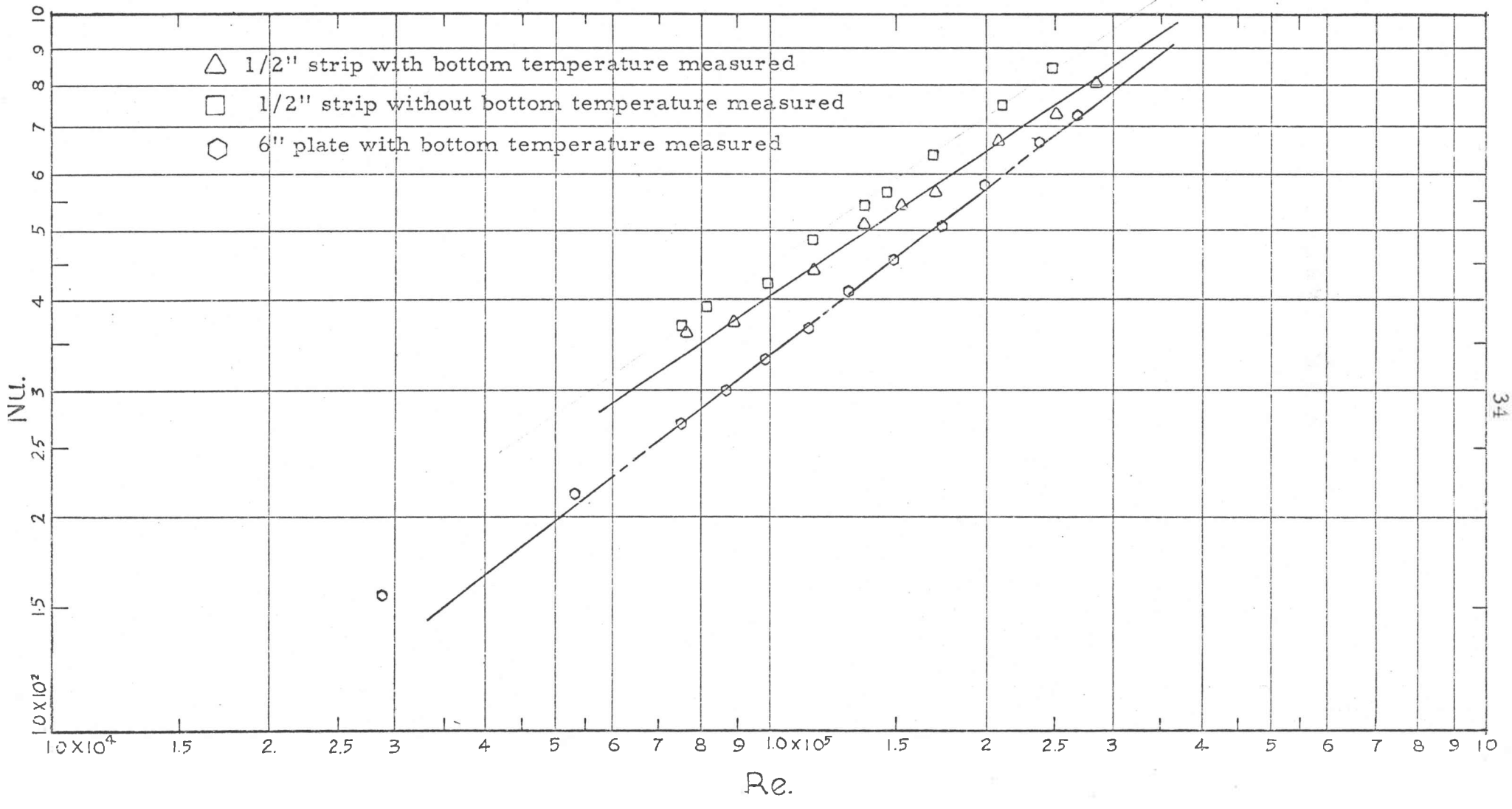

Fig. 18.--Forced convection correlation on 1/2 inch strip, turbulent flow

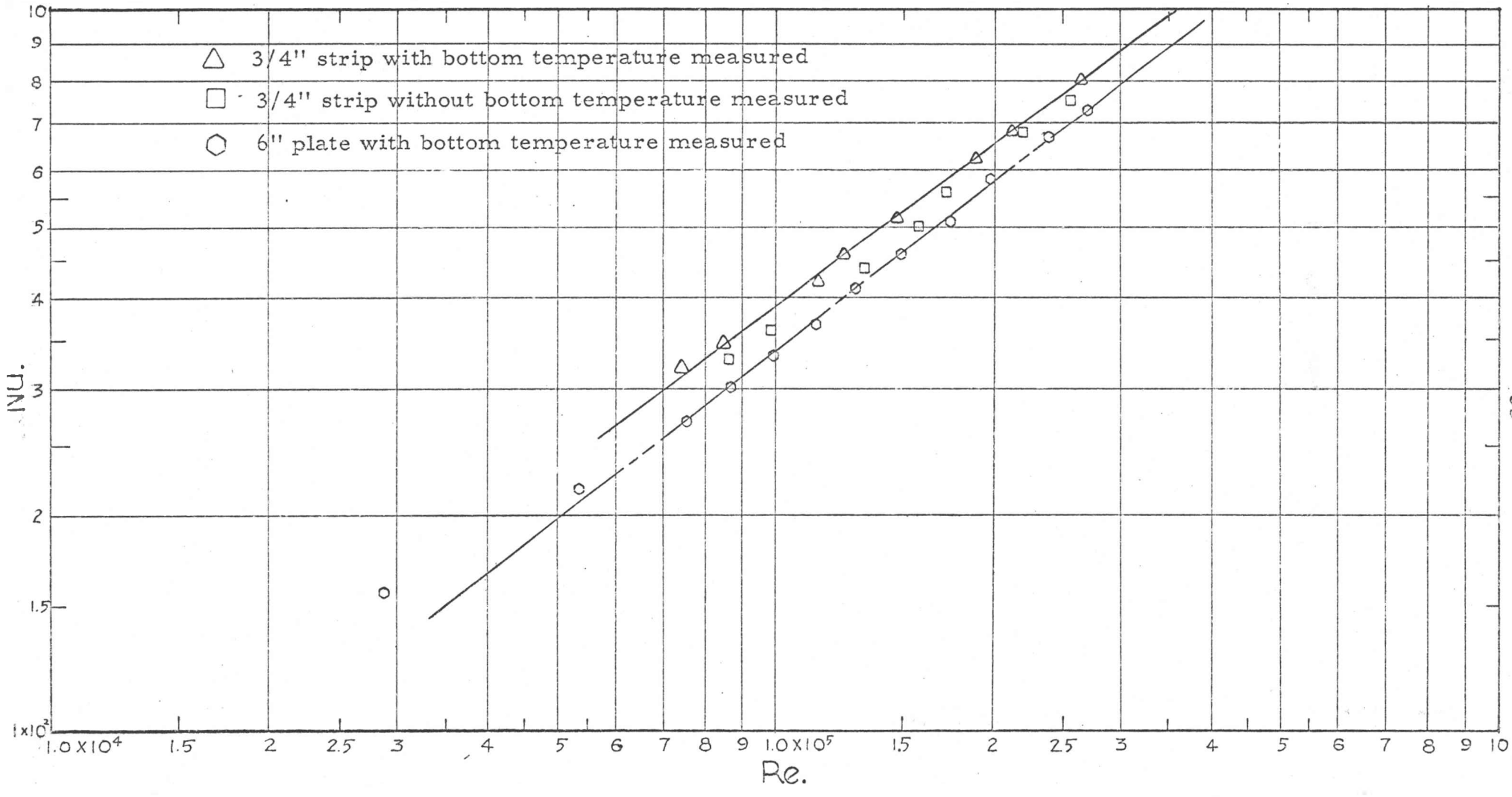

Fig. 19.--Forced convection correlation on 3/4 inch strip, turbulent flow

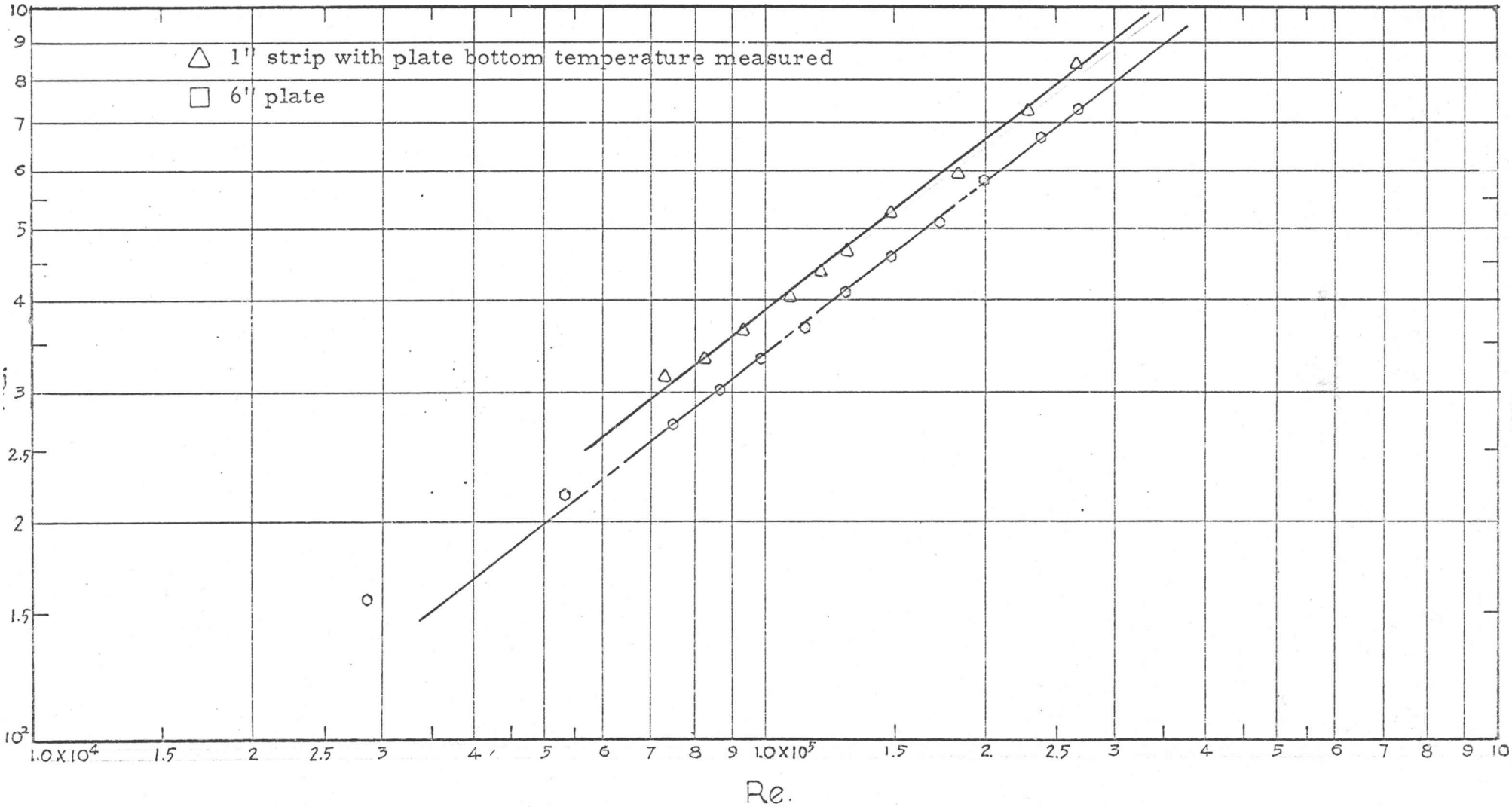

Fig. 20.--Forced convection correlation on 1 inch strip, turbulent flow

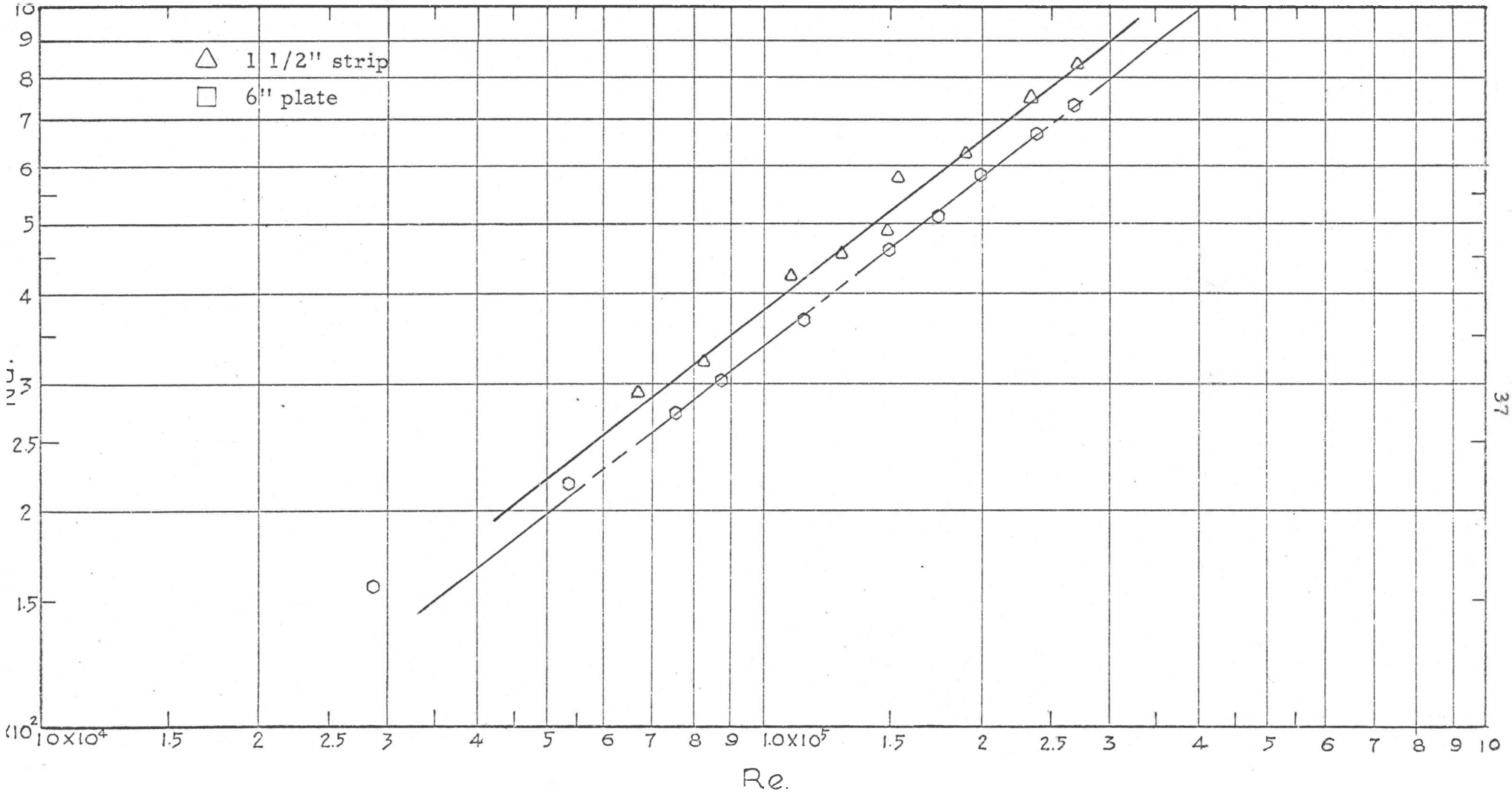

Fig. 21.--Forced convection correlation on 1 1/2 inch strip, turbulent flow

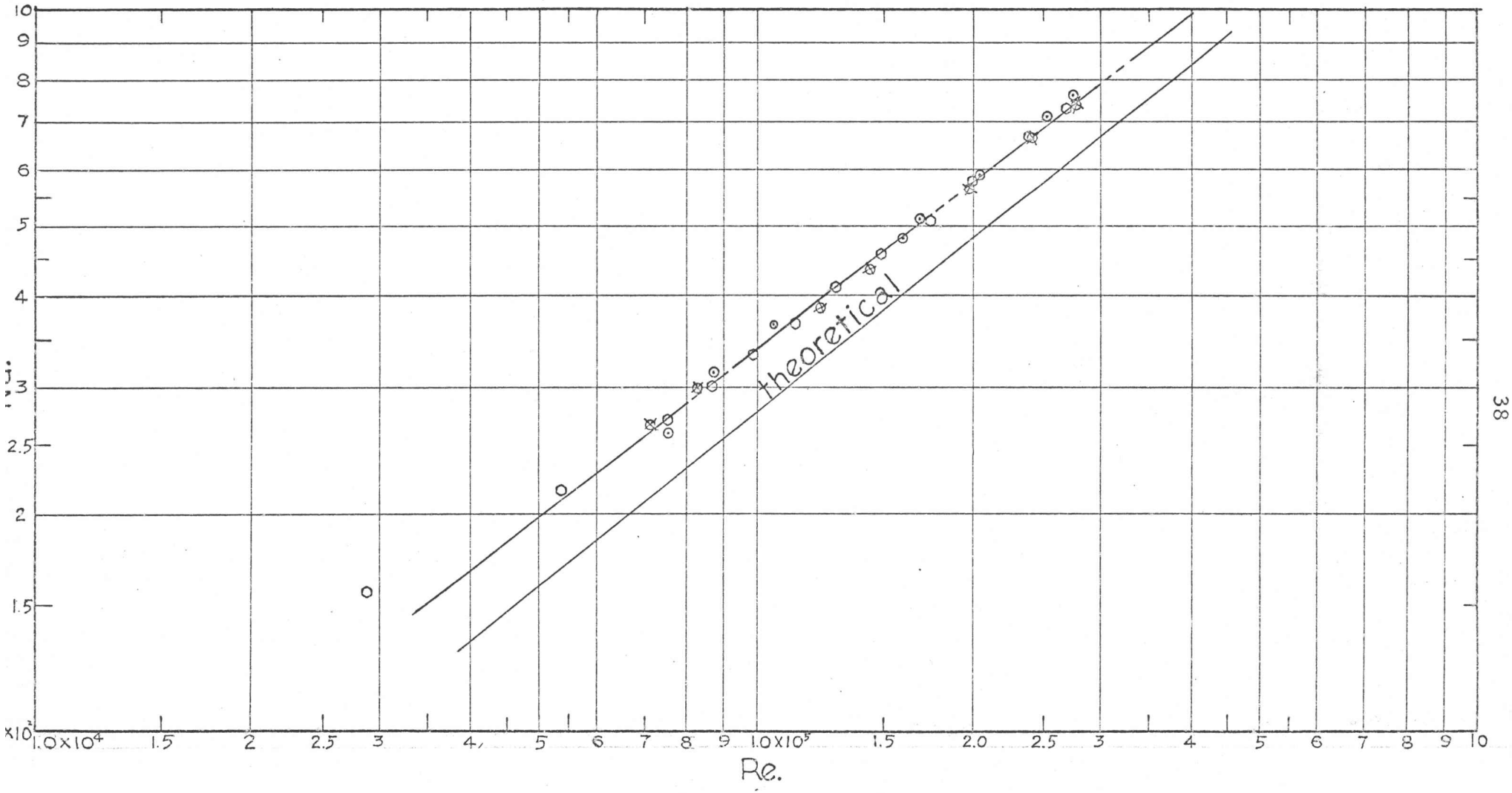

Fig. 22. --Forced convection correlation on 6 inch square plate, turbulent flow

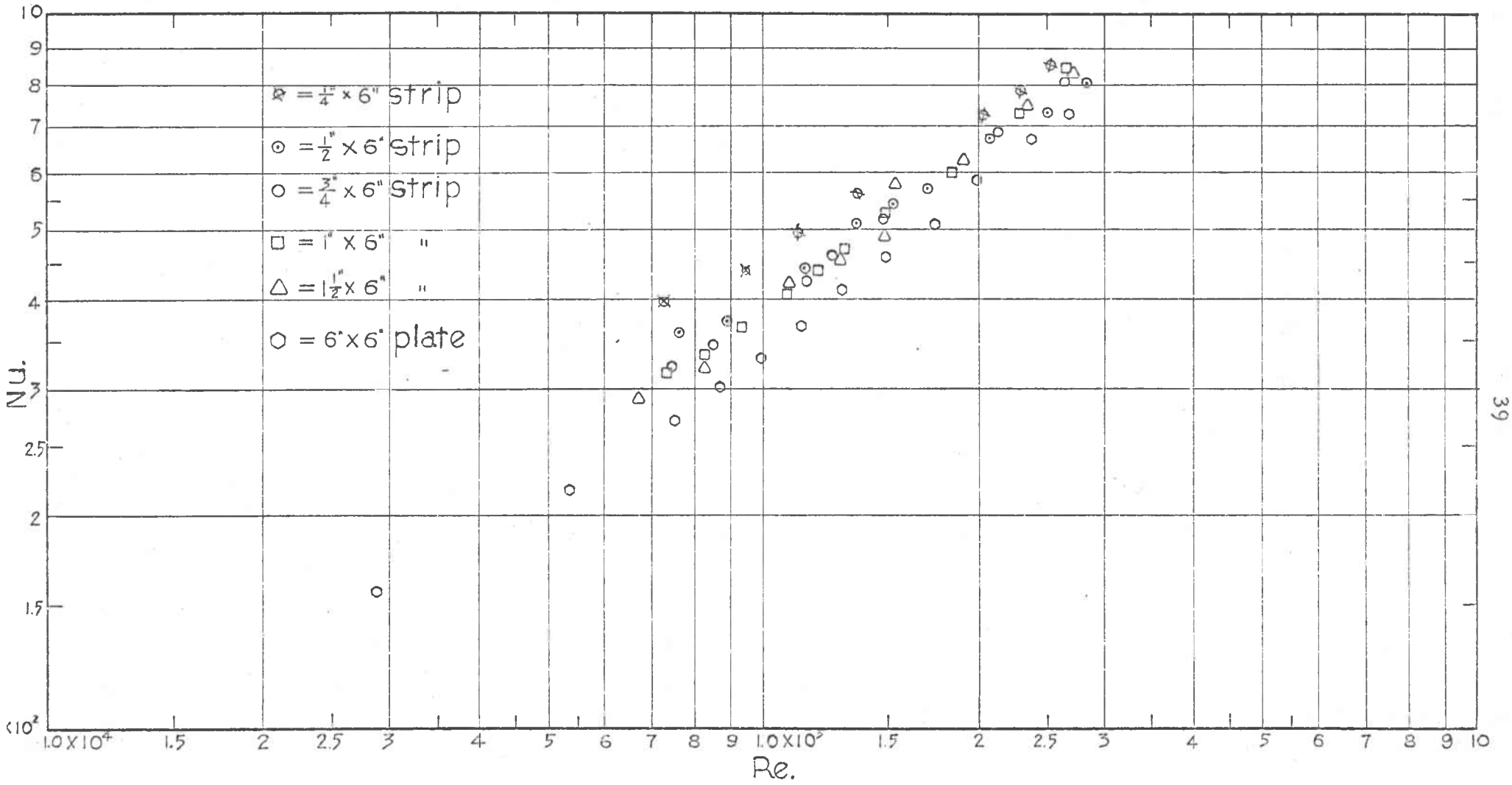

Fig. 23. --Comparison of the forced convection correlation on plate and strips, turbulent flow

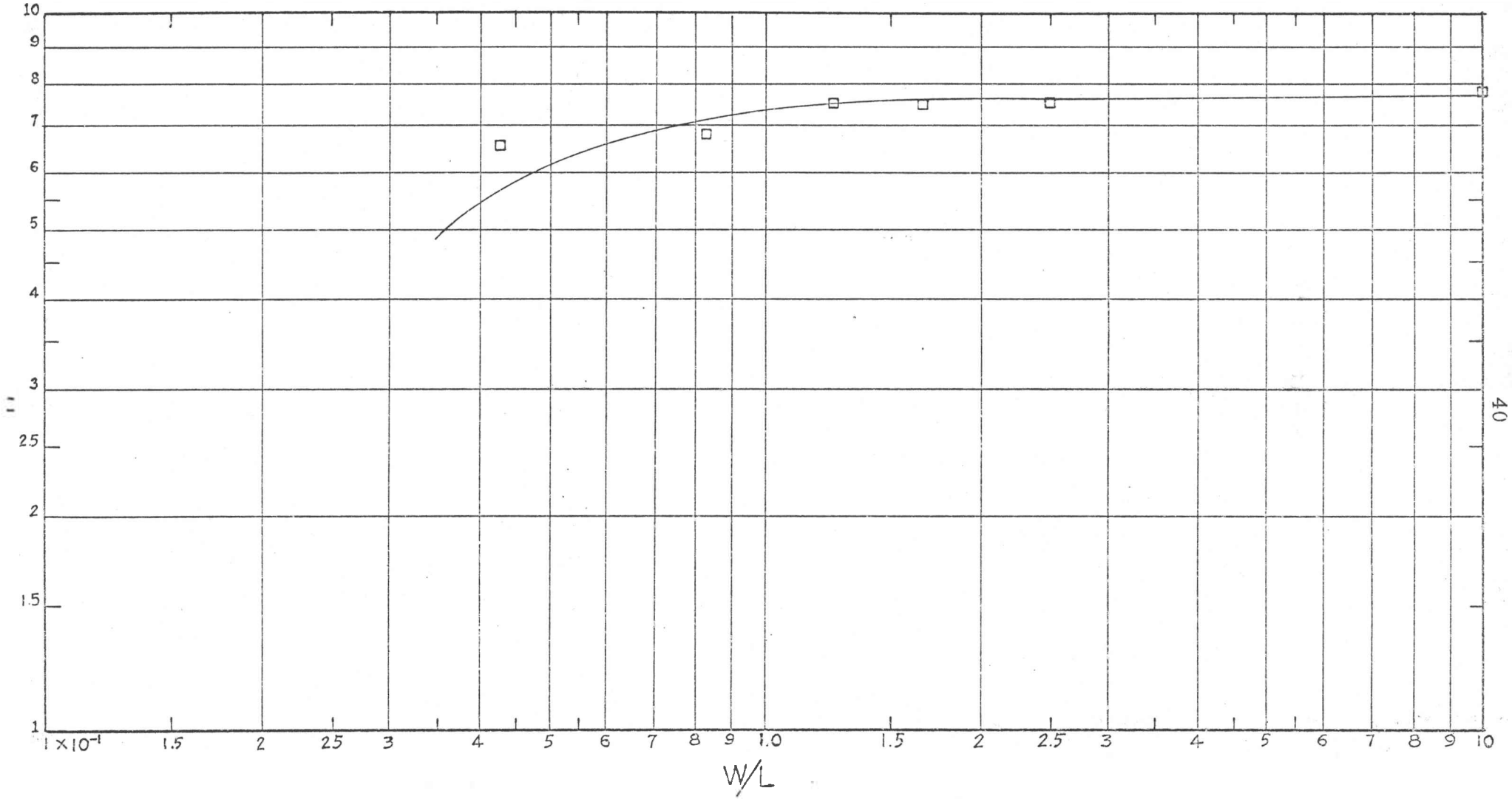

Fig. 24. --Variation of slope of the Nusselt number-Reynolds number correlation with aspect ratio

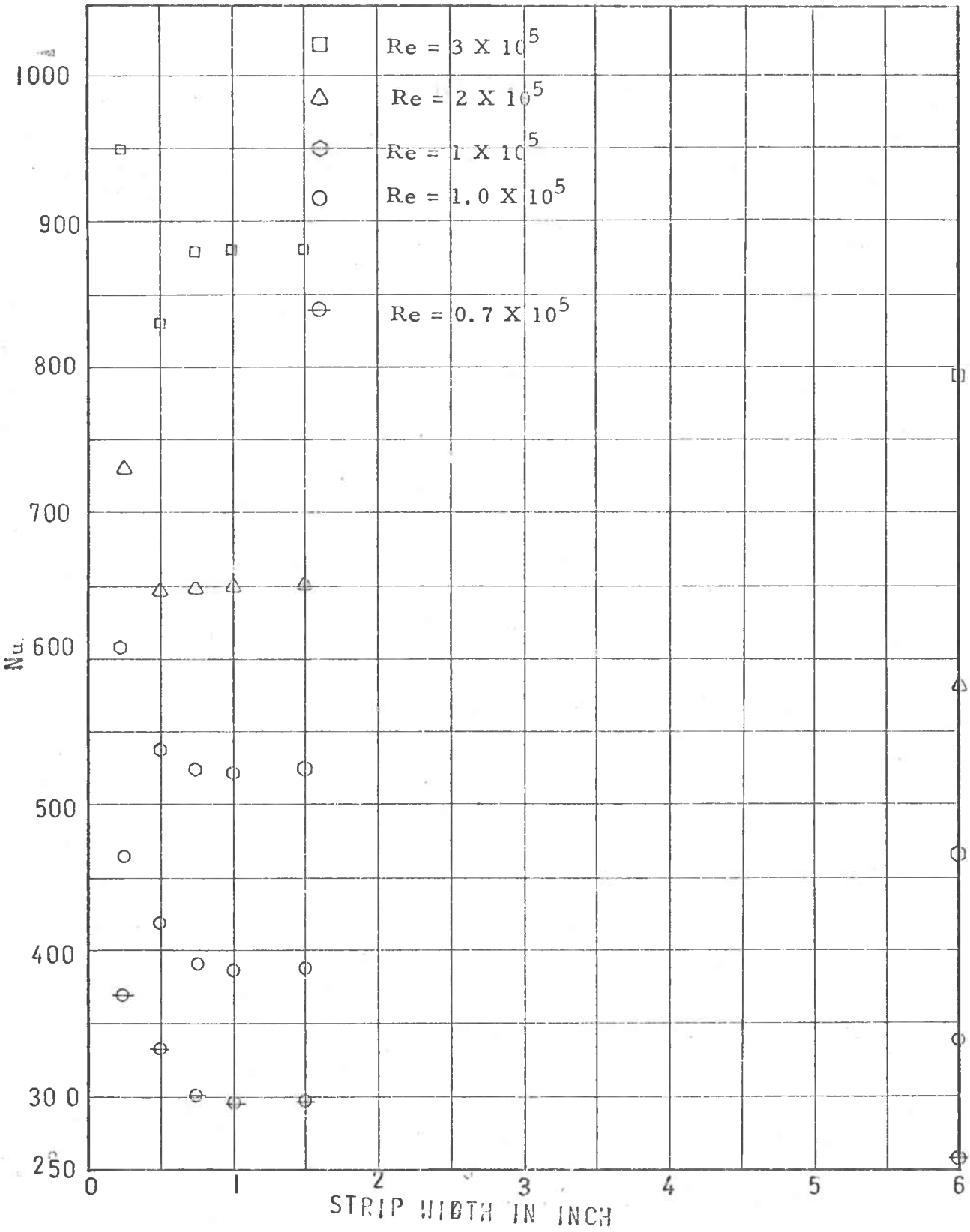

Fig. 25.--Correlation of Nusselt number with strip width

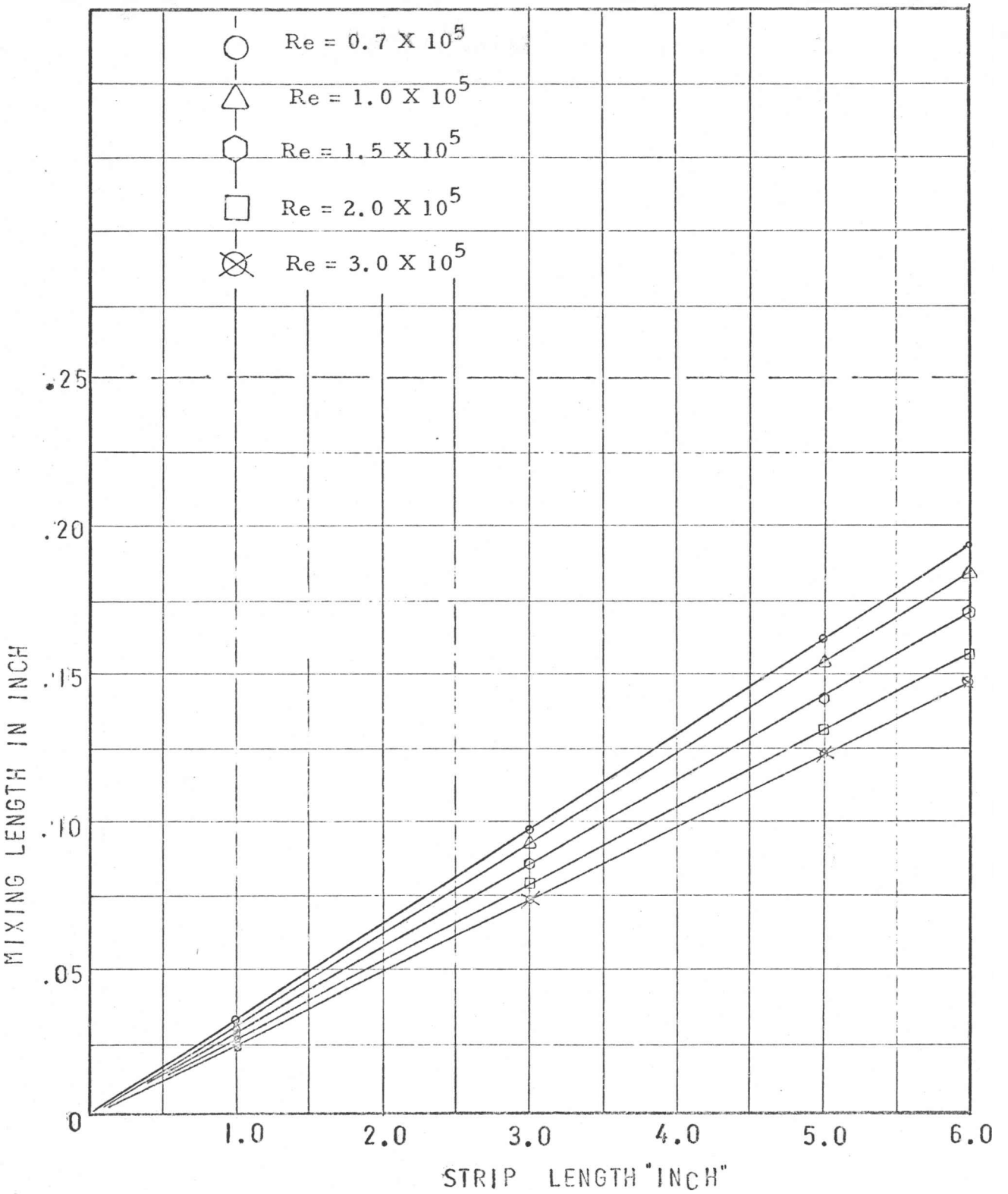

Fig. 26.--Correlation of Prandtl mixing length with strip length

$$St_x Pr^{0.4} = 0.0295 Re_x^{-0.2} \left[1 - \left(\frac{\xi}{x}\right)^{\frac{9}{10}}\right]^{-\frac{1}{9}}$$

Fig. 24 and Fig. 25 illustrate the change in the slope of the Nusselt number-Reynolds number correlation for increasing aspect ratio, respectively.

Figures 17 through 21 indicate that with the Reynolds number held constant, a decrease of aspect ratio results in an increase of the heat transfer coefficient. Take for instance, with Reynolds number held constant, at 1×10^5 and having the 6 inch square plate as standard for comparison, the increase of heat transfer coefficients corresponding to 1/4 inch, 1/2 inch, 3/4 inch, 1 inch and 1 1/2 inch strips are 34 per cent, 25 per cent, 20 per cent, 19 per cent and 19 per cent respectively. This verifies the prediction the author made in the introduction that the edge effect promotes heat convection.

After a close examination of Fig. 24, it is seen that the slope of the Nusselt number-Reynolds number correlation for strips having small aspect ratio is not as large as that for a flat plate. As the aspect ratio increased the curve has the tendency to approach the value of flat plate asymptotically. We can interpret from Fig. 24 that the narrower the strip, that is the smaller the aspect ratio, the more significant is the edge effect. This agrees well with Reynolds analysis (11) (12) of turbulent and laminar heat transfer in circular tube with variable circumferential heat flux as shown in Fig. 3. The explanation of this phenomonan may be partially explained by Prandtl's Mixing

Length Theory.

Under the assumption that momentum of flow is a transport quantity and the momentum and energy transfer in turbulent flow are transported by the same mechanism, Prandtl arrived at an expression for the eddy diffusivity of heat as

$$\epsilon_m = \epsilon_H = "l" \frac{du}{dy} \qquad (2)$$

Here "l" is the mixing length in a direction normal to the plate. If it is assumed that trubulence is isotropic then "l", the mixing length, should be the same in all three coordinate directions. Then "l" can be interpreted as the distance the eddies move in the transverse direction which would transport energy away from the edge of the heated strips.

For constant free stream velocity flow over an external surface, the mixing length can be found by the following equations given in Kays (1):

$$\delta = \frac{\delta_2}{0.097}$$

$$\delta_2 = 0.037 Re^{-0.2} x$$

where δ_2 is the momentum thickness and δ is the boundary layer thickness.

Assuming $"l" = k\delta$

where $k = 0.4$

we have $"l" = 0.153 Re^{0.2} x \qquad (3)$

The mixing length "l" along the longitudinal edge of the strips of the present study was calculated at a distance from the wall equal to the boundary layer thickness. The results are presented in Fig. 26 showing twice the mixing length as a function of strip length. The dash line in Fig. 26 is the 1/4 inch width strip.

The significance of the 2L versus L plot is that the area covered by the transverse mixing length is 38.6 per cent, 19.3 per cent, 12.9 per cent, 9.65 per cent, 6.54 per cent and 1.61 per cent of the 1/4 inch, 1/2 inch, 3/4 inch, 1 inch and 1 1/2 inch strips and the 6 inch square plate, respectively. Since the eddy diffusivity for heat transfer is related to the Prandtl mixing length as given in Equation (2), it is evident that the more the heated surface area covered by the eddies the higher will be the transverse energy removal from the heated strips. This helps to explain why the narrower the strip the higher the heat transfer rate.

Further investigation the "l" -L curve indicated that as the width of the strip narrows while the Reynolds number is held constant, the strip width will soon reach a value over which the eddies occuring in the turbulent flow will be greater than the width of the strip and the flow will become more similar to that perpendicular to the longitudinal axis. This reflects the analogy to the experiment of heat transfer in the flow of a fluid parallel to a wire performed by Mueller as presented in Jakob (3).

Data in Fig. 26 shows that the lower the Reynolds number the more significant is the transverse mixing length effect. For the narrower strips the transverse mixing length effect causes a significantly higher increase in heat transfer at lower Reynolds number than at high Reynolds numbers. This would help to explain why the slope of the Nusselt number-Reynolds number curve is less for the narrower strips. It appears that at a sufficently high Reynolds number the curves may all approach each other with no edge effect present.

Fig. 25 is a plot of Nusselt number as a function of aspect ratio. It shows that the effect of the width of the strip on the Nusselt number is not a smooth continuous curve but seems to flatten in the range of 3/4 inch to 1 1/2 inch widths. This was rechecked experimentally several times and seemed to be reproduceable. It is not clear why this occurs but perhaps it is also related to the transverse eddy motion.

The comparison between the empirical results and the theoretical solution of the 6 inch square plate in Fig. 22 indicates that the experimental results are about 20% higher. This difference may be partly caused by the uncertainty in the effective starting point of the turbulent boundary layer. This part of the experiment was rerun more than three times in different conditions but the results were consistant. Because of the reproducibility of the experimental results, this leads the author to believe that the results presented

here are reliable and correct.

CHAPTER VII

CONCLUSION AND RECOMMENDATIONS

In reviewing this experimental work, one general and significant fact has been firmly established. The edge effect does affect the forced convective heat transfer and the increase is inversely related to the aspect ratio of the strips. In the range of Reynolds number tested the effect is more significant at low Reynolds numbers than at sufficiently high Reynolds numbers.

Based upon the experience gained by the author in performing the experiment the following recommendations are made for improvement of the apparatus in a future experimental program:

1. To eliminate the effect of room temperature fluctuations, further experiments should be performed in a well controlled temperature room.

2. In further experimental work such as described in this thesis, an insulation material having a smooth finishing surface such as a plastic should be used instead of foam. This will give a better surface contact and surface condition as well.

3. The wind tunnel should have a bigger range of speed. This

would allow a wider range of investigation.

4. A Hotwire anemometer should be used to check the turbulence phenomenon.

APPENDIX

APPENDIX A

VELOCITY INVESTIGATION

Seeing that flow stream plays an important role in the field of forced convection heat transfer, a study of the up-stream and down-stream air flow distribution in the test section of the wind tunnel was made to examine the stability of air flow. This study was made by means of two pitot tubes and an inclined manometer. The pitot tubes were vertically inserted into the air stream with the head axis aeligned along the wind direction and the open ends connected to the inclined manometer in order to measure the dynamic pressure. The velocity profiles of the air flow in the test section having test sample mounted on are illustrated in Fig. 27. The results indicate that the air flow in the wind tunnel was uniform enough for this research program. The conversion of the dynamic pressure to velocity was made through equation

$$V = \sqrt{\frac{2g\Delta h\gamma}{\rho_{air}}}$$

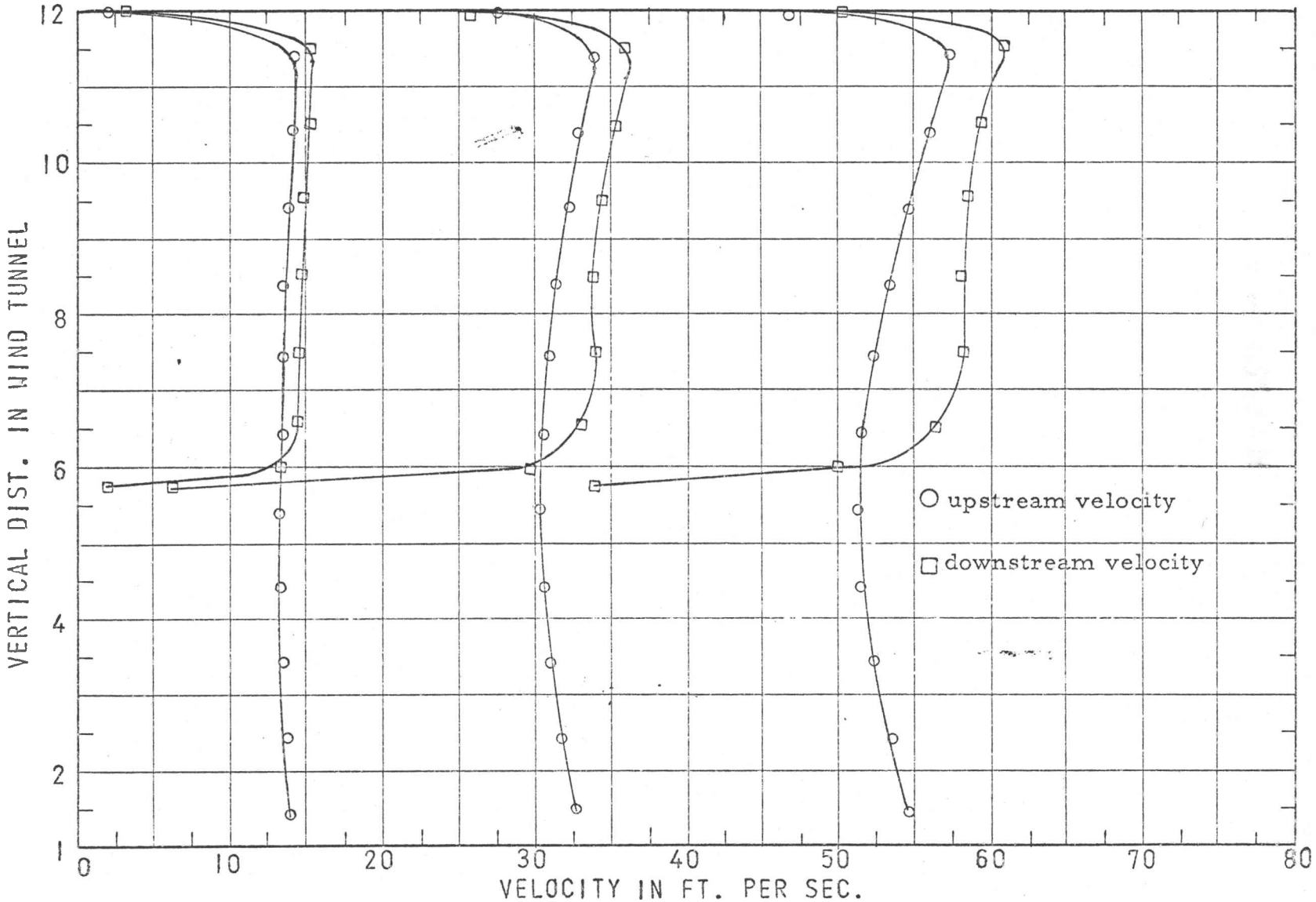

Fig. 27.--Velocity distribution

APPENDIX B

UNCERTAINTY ANALYSIS

In order to determine the accuracy of this experiment an uncertainty analysis was conducted to determine possible error that could have been encountered in this experiment.

The calculated uncertainty based on the author's adjustment and the Kline and McClintock (17) method,

$$\omega_R = \left[\left(\frac{\partial R}{\partial V_1}\omega_1\right)^2 + \left(\frac{\partial R}{\partial V_2}\omega^2\right)^2 + - - - + \left(\frac{\partial R}{\partial V_n}\omega_n\right)^n \right]^{\frac{1}{2}}$$

where ω_R = uncertainty interval

R = linear function of n independent variables

ω_i = maximum deviation of the i^{th} variable from its mean

is $\pm$ 4.5 per cent for Reynold number and $\pm$ 4.4 per cent for Nusselt number. This could certainly increase or decrease the empirical result as compared with the theoretical value as indicated in Fig. 22.

APPENDIX C

REYNOLD NUMBER CALCULATION

The general equation for finding the Reynolds number is

$$Re_x = \frac{\rho_\infty U_\infty l}{\mu}$$

Since both ρ_∞ and μ are functions of temperature and the temperature in this experiment was not constant, using ρ_∞ and μ as constant values will lead to error. Thus, a simplified general equation to find the Reynolds number was worked out as follows:

$$Re_x = 8.305 \left(\frac{h \rho_\infty}{\mu}\right)^{\frac{1}{2}}$$

with $$U_\infty = 16.61 \left(\frac{h}{\rho_{air}}\right)^{\frac{1}{2}}$$

and $$\rho_\infty = 0.01878 \left(\frac{P_\infty}{T}\right)^{\frac{1}{2}}$$

where P_∞ = Free stream pressure in the test section

= 70.73 h_{Hg} (barometer reading) - 0.827h X5.2

μ = viscosity of air at room temperature

h = manometer reading, inch, Merian Red oil

NUSSELT NUMBER CALCULATION

The Nusselt number was calculated as follows; The temperature used for the heat conduction loss calculation was the plate temperature in ^{o}F, and the Temperature used for finding the radiation heat loss was the plate temperature in ^{o}R.

$$Nu = \frac{hL}{k}$$

with $$h = \frac{q}{A(\Delta T)}$$

and $$A = LW$$

The Nusselt number was reduced to

$$Nu = \frac{q}{kA(\Delta T)}$$

where q was the net heat loss through convection and was defined as

$$q = q_{in} - q_{\text{conduction and radiation heat loss.}}$$

The conduction heat loss was found by the following equation

$$q_{\text{conduction loss}} = kS \Delta T$$

where k = thermal conductivity of air

$= 0.0112$ BTU/hr-ft-^{o}F

and S is the geometric shape factor of the foam and was calculated

from the following equation

$$S = 12(\text{recess width}) + 1.65(\text{recess perimeter})$$

The derivative of the above equation was given in Appendix D.

The radiation heat loss was found by the following equation

$$q_{\text{rad. loss}} = A_p \sigma (T_p^4 - T^4)$$

where A_p = plate surface area

σ = Stefan Boltzmann constant

$= 0.1714 \times 10^{-8}$ BTU/hr-ft^2 -$^\circ$R^4

T_p = plate temperature in $^\circ$R

T_∞ = ambient temperature in $^\circ$R

The justification of the above equation was based on the assumption that the surroundings were a black body.

APPENDIX D

SHAPE FACTOR MEASUREMENT

The shape factor of the insulation foam plate used in this experiment was measured by means of an electrical conductive paper analog. The analog consisted of a scale conductive paper model and a rectangular conductive paper model as shown in Fig. 15. Assuming a unit depth, the shape factor of the rectangular conductive paper model was calculated from

$$S_1 = \frac{\text{length}}{\text{width}} \qquad (1)$$

and was used as a standard for comparison. The simulated constant temperature boundaries of the conductive medium were obtained by applying copper wires and highly conductive silver paint to the edge of the model. Having the electrical resistance across the boundaries of the models measured by means of an ohmmeter the shape factor of the conduction medium was calculated by the following relationship

$$\frac{S_1}{S_2} = \frac{R_2}{R} \qquad (2)$$

where S_1 = Shape factor

R_1 = Electrical resistance

Equation (1) was derived based on the analogy between heat flow and electrical current flow. That is, the heat flow through a thermal resistance is analogous to the flow of current through an electrical resistance.

The conductive paper electrical analog model of the insulating foam plate having a 6 inch by 6 inch by 1/4 inch recess is shown in Fig. 28. The discontinuous gap shown in the figure simuh ted the temperature discontinuous between the foam and the heated plate. The measured value of the shape factor was

$$S_{total} = 7.65$$

The equal potential field plot, as shown in Fig. 16. indicated that only a narrow distance from the recess edge was significant to conduction heat less through the four edges. Thus the system could be considered a two dimensional and the total measured shape factor for this could be justified as

$$S_{total} = S_{base} + S_{edge}$$

The shape factor of the base was

$$S_{has} = \frac{6}{1}$$

$$= 6$$

subtracting the base shape factor from the total we get

$$S_{edge} = 1.65$$

Based upon the above measured values and the unit depth assumption the general equation for finding the shape factor of the

whole plate was derived as

$$S_{total} = 12 \text{ (recess width)} + 1.61\text{(recess perimeter)}$$

The dimensions of the width and the perimeter are in feet.

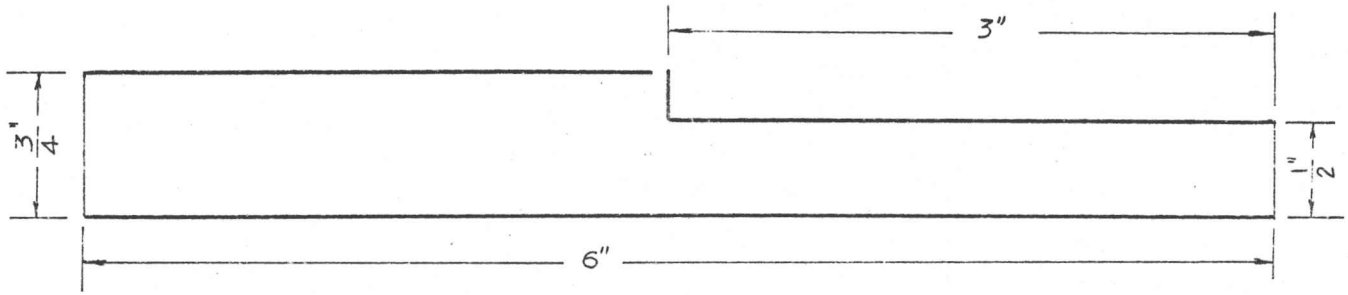

Fig. 28.--Electrical conductive paper model

TABLE I

1/4" X 6" STRIP POWER IN 2.08 WATT $\bar{P}$ = 25.57"Hg. $\bar{T}$ = 81.9°F

U	Re_L	q	$T_o - T$	$Nu_{L.C.P.}$	Nu_L
ft/sec.	X 10^5	BTU/hr.	°F	$\frac{hL}{k}$	$\frac{T_o}{\bar{T}}^{0.5} Nu_{LCP}$
28.60	0.719	5.85	50.05	372.0	395.0
34.00	0.924	6.28	47.42	420.5	438.5
44.45	1.105	6.25	41.11	481.0	498.5
49.90	1.240	6.27	38.48	526.0	545.0
55.20	1.360	6.37	35.48	544.0	561.0
62.50	1.550	6.48	32.65	627.0	646.0
77.70	1.940	6.51	29.27	702.0	720.5
90.60	2.235	6.50	26.95	762.0	780.5
100.50	2.470	6.56	24.13	851.0	870.5

TABLE II

1/2" X 6" STRIP POWER IN 3.82 WATT $\bar{P}$ = 25.3"Hg. $\bar{T}$ = 77.0°F

U	Re_L	q	$T_o - T$	$Nu_{l.c.p.}$	Nu_L
ft/sec	X 10^5	BTU/hr.	°F	$\frac{hL}{k}$	$\frac{T_o}{T}^{0.5} Nu_{LCP}$
30.40	0.766	11.424	55.38	339.0	361.0
34.78	0.890	11.520	51.50	356.0	372.0
45.85	1.160	11.708	43.88	425.0	441.0
53.50	1.349	11.832	38.13	495.0	512.5
59.50	1.502	11.915	36.05	526.0	542.2
66.90	1.694	11.968	34.65	549.5	566.0
82.10	2.070	12.090	29.33	656.0	673.0
96.50	2.479	12.135	27.16	711.0	728.0
111.00	2.840	12.198	24.55	790.0	807.0

TABLE III

3/4" X 6" STRIP POWER IN 3.915 WATT $\bar{P}$ = 25.48"Hg. $\bar{T}$ = 76.75°

U	Re_L	q	$T_o - T$	$Nu_{L.C.P.}$	Nu_L
ft/sec.	X 10^5	BTU/hr.	°F	$\frac{hL}{k}$	$\frac{T_o}{T}^{0.5} Nu_{LCP}$
29.40	0.740	12,000	41.49	307.0	320.0
33.76	0.851	12,103	38.27	336.0	348.0
44.30	1.115	12,314	32.28	404.0	414.5
49.30	1.241	12,418	29.05	453.0	465.0
58.80	1.480	12,516	26.00	508.0	520.0
76.00	1.917	12,664	21.53	624.0	634.5
86.00	2.164	12,713	19.95	676.0	688.0
100.64	2.633	12,797	17.53	790.0	802.6

TABLE IV

1" X 6" STRIP POWER IN 5.72 WATT $\bar{P}$ = 25.44"Hg. $\bar{T}$ = 80.7°F

U	Re_L	q	$T_o - T$	$Nu_{L.C.P.}$	Nu_L
ft/sec.	X 10^5	BTU/hr.	°F	$\frac{hL}{k}$	$\frac{T_o}{T}^{0.5} Nu_{LCP}$
29.39	0.733	17,648	48.36	290.0	315.0
33.05	0.825	17,780	44.60	318.0	332.0
37.70	0.935	17,920	40.93	350.2	363.0
44.20	1.095	18,094	36.47	396.0	409.0
48.30	1.195	18,170	33.95	427.0	440.0
52.40	1.300	18,150	31.90	455.0	467.5
59.20	1.487	18,280	28.20	511.0	525.0
73.70	1.850	18,198	24.44	583.0	596.0
93.80	2.355	18,357	20.20	723.0	735.0
106.50	2.660	18,447	17.65	832.0	840.0

TABLE V

1 1/2" X 6" STRIP POWER IN 7.63 WATT $\bar{P}$ =25.56"Hg $\bar{T}$ =72.0°F

U	Re_L	q	$T_o - T$	$Nu_{L.C.P.}$	Nu_L
ft/sec.	X 10^5	BTU/hr.	°F	$\frac{hL}{k}\left(\frac{T_o}{T}\right)^{0.5}$	Nu_{LCP}
26.1	0.672	23.995	45.28	279.0	293.0
31.4	0.832	24.120	40.80	311.0	322.0
43.0	1.105	24.547	32.00	415.0	426.5
50.2	1.291	24.670	29.40	442.0	454.0
58.7	1.515	24.750	27.56	474.0	588.0
74.1	1.904	25.050	21.25	622.0	634.5
92.7	2.365	25.270	19.36	735.0	746.0
106.5	2.730	25.235	17.40	835.0	845.0

TABLE VI

6" X 6" PLATE POWER IN 30.4 WATT $\bar{P}$ = 25.5"Hg. $\bar{T}$ = 74.3°F

U	Re_L	q	$T_o - T$	$Nu_{l.c.p.}$	Nu_L
ft/sec.	X 10^5	BTU/hr.	°F	$\frac{hL}{k}\left(\frac{T}{T_o}\right)^{0.5}$	Nu_{LCP}
11.28	0.290	93.020	85.37	144.0	155.0
21.00	0.539	95.739	58.43	219.0	231.0
29.20	0.754	96.139	49.35	260.0	272.0
33.80	0.874	97.562	45.28	288.0	301.0
38.40	0.992	98.136	43.05	322.5	335.0
44.30	1.150	98.692	40.93	357.0	369.5
51.00	1.300	99.250	32.70	405.0	416.5
58.20	1.510	99.61	30.17	441.5	454.0

SELECTED BIBLIOGRAPHY

1. Kays, W. M. Convective Heat and Mass Transfer. New York: McGraw Hill, 1966.

2. Schlichting, Hermann. Boundary Layer Theory. New York: McGraw Hill Book Company, 1951.

3. Jakob, Max. Heat Transfer, Volume I. New York: John Wiley and Sons, Inc., 1940.

4. Holman, J. P. Heat Transfer. New York: McGraw Hill Book Company, 1963.

5. Goldstein, S. Modern Development in Fluid Dynamics, Volume I and Volume II. New York: Dover Publications Inc., 1965.

6. Knudsen, James G. and Katz, Donald L. Fluid Dynamics and Heat Transfer. New York: McGraw Hill Book Company, 1958.

7. Sogin, H. H. "Laminar Transfer from Isothermal Spanwise Strips on Flat Plate," Journal of Heat Transfer, (February, 1960), 53-62.

8. Sogin, H. H. and Goldstein, R. J., "Turbulent Transfer from Isothermal Spanwise Strips on Flat Plate", (Boulder, Colorado), 1961.

9. Rannie,W. D. "Heat Transfer in Turbulent Shear Flow," Journal of the Aeronautical Sciences, (May, 1956), 485-489.

10. Cess, R. D., "Heat Transfer to Laminar Flow Across a Flat Plate with a Nonsteady Surface Temperature," Journal of Heat Transfer, Transaction of the A.S.M., (August, 1961), 274.

11. Reynolds, W. C., "Heat Transfer to Fully Developed Laminar Flow in a Circular Tube with Arbitrary Circumferential Heat Flux," Journal of Heat Transfer, Transaction of the A.S.M.E., LVII (1960) 1-5.

12. Reynolds, W. C., "Turbulent Heat Transfer in a Circular Tube with Variable Circumferential Heat Flux," International Journal of Heat and Mass Transfer, VI (1963), 445-454.

13. Sparrow, E. M. and Lin, S. H., "Turbulent Heat Transfer in a Tube with Circumferential Varying Temperature," International Journal of Heat and Mass Transfer, VI, (1963) 866-867.

14. Black, A. W. and Sparrow, E. M., "Experiments on Turbulent Heat Transfer in a Tube with Circumferential Varying Thermal Boundary Conditions," Journal of Heat Transfer, Transactions of the A.S.M.E. (August, 1967) 258-2268.

15. Bingham, Bruce D., "A Study of the Mode of Transfer of Metabolic Heat from a Biological System to the Local Surrounding," Master Thesis unpublished, Brigham Young University 1968.

16. Lin, Philip T., "A Study of Turbulent Heat Transfer from Smooth and Rough Flat Plate Surfaces," Unpublished master thesis, Brigham Young University, 1969.

17. Kline, S. J., and McClintock, F. A., "Uncertainties in Single-Sample Experiments", Mechanical Engineering, (January, 1953)

ABSTRACT

ABSTRACT

This thesis was an experimental study of turbulent heat transfer over a flat plate having transverse temperature variation. This study was accomplished by means of five uniformly resistance-heated strips of the same length but different aspect ratio, each embedded flushly into an insulation foam plate to simulate the plate with transverse step temperature change. The experiment was performed in a subsonic wind tunnel.

The results of this study indicated that under constant Reynolds number, the heat transfer coefficient or Nusselt number increased as the width of the strip decreased. At higher Reynolds number, the increase in Nusselt was not as large as it was at lower Reynolds number.

APPROVED: